PEOPLE’S DEMOCRATIC REPUBLIC OF ALGERIA
MINISTRY OF HIGHER EDUCATION AND RESEARCH SCIENTIST
MOHAMED BOUDIAF UNIVERSITY- M’SILA

FACULTY OF TECHNOLOGY
ELECTRONICS DEPARTMENT
N° :......................................

FIELD: SCIENCE AND TECHNOLOGY
FILLIARY: ELECTRONICS
OPTION: INSTRUMENTATION

Thesis presented for the award of
Academic Master's degree
by:
MAHDID Sabah

Title

Solar Energy Prediction using PSO_SVR
- Case study Adrar site -

Jury members:

Dr: Djerioui Mohamed	University of M'sila	Chairman
Mr: Mezaache Hatem	University of M'sila	Reporter
Dr: Zemouri Nahed	University of M'sila	Co-Rapporteur
Dr: Fodil Malika	University of M'sila	Examiner

Academic year: 2024 / 2025

ACKNOWLEDGEMENTS

First and foremost, I thank and praise Allah Almighty for granting me the strength, patience, and determination to complete this work.

I would like to express my sincere gratitude to my supervisors, Mr. Hatem Mezaache and Dr. Nahed Zemouri, for their valuable guidance, constant support, and availability throughout the preparation of this thesis.

I also thank the members of the jury for honoring me by accepting to evaluate this work and for their constructive comments and suggestions.

Finally, I express my deep appreciation to everyone who supported me, whether directly or indirectly, during this academic journey.

DEDICATION

To those who instilled in me the meaning of strength and patience.
To those who called me at every moment, and accompanied me with prayer and hope...
To my dear parents, I dedicate this note as a token of gratitude and gratitude.
To my dear siblings, you are the true support, the joy of childhood, and the companions of the path...
Thank you for your irreplaceable presence.
And to my dear friends and companions of the road.
I dedicate these pages to you, who witnessed a dream that was realized with your presence around me.

Résumé

L'intégration des sources d'énergie renouvelable dans le mix énergétique est cruciale pour la transition vers une économie à faibles émissions de carbone. Parmi ces sources, l'énergie solaire occupe une place importante en raison de sa disponibilité et de son potentiel à fournir une énergie propre et renouvelable. Cependant, le caractère intermittent et variable de la production d'énergie solaire engendre des défis majeurs pour la gestion et la stabilité des réseaux électriques

Ce travail propose une approche innovante pour l'estimation de la puissance solaire à différents horizons, en combinant des techniques d'optimisation avancée et de machine learning. L'optimisation par essaim de particules (PSO) est utilisée pour ajuster efficacement les hyper-paramètres de la régression à vecteurs de support (SVR), en améliorant ainsi la précision des estimations. Cette méthode permet de mieux capter les variations de la production solaire en fonction des conditions météorologiques et temporelles, offrant une solution performante et adaptable pour les applications de prévision énergétique.

Pour évaluer notre système d'estimation deux méthodes d'évaluation sont employées, une évaluation statistique basée sur les indicateurs de performance tels que l'erreur quadratique moyenne (RMSE), l'erreur absolue pourcentage moyenne (MAPE), et le coefficient de détermination (R^2), ainsi qu'une évaluation graphique utilisant des nuages de points pour comparer les données réelles aux résultats prédits, ces méthodes d'évaluation permettant de comparer les prédictions aux valeurs réelles et de vérifier l'efficacité de l'approche hybride proposée.

Mots clés — Estimation, Puissance solaire, entrées météorologiques, PSO, SVR.

Abstract

The integration of renewable energy sources into the energy mix is crucial to the transition to a low-carbon economy. Among these sources, solar energy occupies an important place due to its availability and potential to provide clean, renewable energy. However, the intermittent and variable nature of solar power generation creates major challenges for the management and stability of power grids.

This work proposes an innovative approach for estimating solar power over different time horizons, combining advanced optimization and machine learning techniques. Particle swarm optimization (PSO) is used to efficiently adjust the hyper-parameters of support vector regression (SVR), thereby improving the accuracy of the estimates. This method better captures variations in solar production as a function of meteorological and temporal conditions, offering a powerful and adaptable solution for energy forecasting applications.

To evaluate our estimation system two evaluation methods are employed, a statistical evaluation based on performance indicators such as root mean square error (RMSE), mean absolute percentage error (MAPE), and coefficient of determination (R^2), as well as a graphical evaluation using scatter plots to compare actual data with predicted results, these evaluation methods allowing to compare predictions with actual values and to verify the effectiveness of the proposed hybrid approach.

Keywords : Estimation, Solar power, meteorological inputs, PSO, SVR.

ملخص:

إن دمج مصادر الطاقة المتجددة في مزيج الطاقة أمر بالغ الأهمية للانتقال إلى اقتصاد منخفض الكربون. ومن بين هذه المصادر، تحتل الطاقة الشمسية مكانة هامة بسبب توافرها وقدرتها على توفير طاقة نظيفة ومتجددة. ومع ذلك، فإن الطبيعة المتقطعة والمتغيرة لإنتاج الطاقة الشمسية تخلق تحديات كبيرة لإدارة واستقرار شبكات الكهرباء.

يقترح هذا العمل نهجًا مبتكرًا لتقدير الطاقة الشمسية على مدى آفاق زمنية مختلفة، يجمع بين تقنيات التحسين المتقدمة والتعلم الآلي. يُستخدم أسلوب تحسين سرب الجسيمات (PSO) لضبط المعلمات المفرطة لانحدار متجه الدعم (SVR) بكفاءة، وبالتالي تحسين دقة التقديرات. تلتقط هذه الطريقة بشكل أفضل الاختلافات في إنتاج الطاقة الشمسية كدالة للطقس والظروف الزمنية، مما يوفر حلاً قويًا وقابلًا للتكيف لتطبيقات التنبؤ بالطاقة.

لتقييم نظام التقدير الخاص بنا تم استخدام طريقتين للتقييم، تقييم إحصائي يعتمد على مؤشرات الأداء مثل جذر متوسط الخطأ المربع(RMSE) ، ومتوسط الخطأ المئوي المطلق(MAPE) ، ومعامل التحديد(R^2) ، بالإضافة إلى تقييم بياني باستخدام مخططات مبعثرة لمقارنة البيانات الفعلية بالنتائج المتوقعة، وتسمح طرق التقييم هذه بمقارنة التنبؤات بالقيم الفعلية والتحقق من فعالية النهج الهجين المقترح.

الكلمات المفتاحية: التقدير، الطاقة الشمسية، مدخلات الأرصاد الجوية، PSO، SVR.

Table of contents

Chapter 1: Renewable Energy and Solar Power

Chapter 2: Support Vector Regression (SVR) and Particle Swarm Optimization (PSO)

Chapter 3: Results and Discussion

LIST OF FIGURES

LIST OF TABLES

Introduction

Introduction

Optimizing renewable energy production systems is a major challenge in the current context of energy transition. Among renewable energy sources, solar power occupies a prominent position due to its abundance and sustainability. However, one of the major difficulties in harnessing it lies in accurately predicting the energy produced, which can vary according to a number of factors such as weather, location and geographical conditions. Thus, reliable estimation of solar energy at different forecast horizons is essential to optimize its integration into energy systems.

Previous work in this field has demonstrated the effectiveness of support vector regression (SVR) for solar energy prediction. The SVR technique enables short-term solar power forecasts to be obtained with high accuracy [1]. In addition, the optimization of model hyper-parameters by advanced optimization techniques, such as particle swarm optimization (PSO), has been shown to be an effective method for improving the performance of prediction models. Integrating optimization methods such as PSO with SVR enables its parameters to be optimized in such a way as to enhance the reliability of solar power forecasts [2].

In this context, the use of machine learning methods such as SVR, combined with high-performance optimization techniques such as particle swarm optimization (PSO), is proving to be a promising approach for improving forecast accuracy. SVR, as a non-linear regression method, efficiently models the complex relationship between the input variables and the output of interest, while PSO, as an optimization algorithm inspired by the behavior of animal swarms, is used here to optimize the SVR hyper-parameters.

The first chapter of this dissertation introduces the fundamental concepts related to renewable energy, with a particular focus on solar power, its advantages and challenges. This chapter also introduces the issues involved in estimating solar power production, an essential area for managing and optimizing energy networks.

The second chapter explores in detail the two main methods used in this study. Support Vector Regression (SVR) is discussed in terms of its theoretical and practical foundations, while Particle Swarm Optimization (PSO) is explained as an effective optimization technique for tuning SVR hyper-parameters and improving the accuracy of its predictions.

Finally, the third chapter presents the results obtained from applying the model to the Adrar site in Algeria. This chapter discusses the performance of the combined SVR-PSO model in terms of solar energy forecast accuracy, and analyzes the practical implications of this approach for energy resource management in this region.

In conclusion, this work aims to propose a robust, high-performance method for improving solar energy forecasts, which could contribute significantly to more efficient management of renewable energy resources. The application of SVR coupled with PSO optimization, particularly in specific regions such as Adrar, represents a significant advance for optimizing energy systems and reducing solar energy uncertainties.

Chapter 1
Renewable Energy and Solar Power

1.Introduction:

The global demand for energy continues to rise in tandem with the growth of the world's population, the acceleration of industrialization, and the rapid advancement of technology. This escalating demand has placed unprecedented pressure on conventional energy sources such as coal, oil, and natural gas—resources that are not only finite but also contribute significantly to environmental degradation. The combustion of fossil fuels is a major source of air pollution and greenhouse gas emissions, exacerbating climate change and its attendant risks to ecosystems and human societies (IPCC, 2023).

In response to the mounting environmental and socio-economic challenges posed by climate change, there is a growing imperative to transition towards cleaner, more sustainable, and renewable energy sources. Advances in technology have progressively enhanced the efficiency with which renewable resources can be harnessed, rendering them increasingly viable alternatives to traditional fossil fuels.

Among the portfolio of renewable energy options, solar energy emerges as one of the most promising. It is abundant, ubiquitous, and environmentally benign, with the potential to meet a significant proportion of global energy needs (IEA, 2024). Solar power not only aligns with the goals of sustainable development but also holds promise in diversifying energy systems and reducing dependence on carbon-intensive fuels.

This chapter provides a comprehensive exploration of renewable energy, with a particular focus on the principles and applications of solar energy. It situates solar energy within the broader context of renewable resources, highlighting its potential contributions to sustainable energy transitions and its relevance to contemporary debates on energy security, environmental protection, and technological innovation.

2.Introduction to Renewable Energy:

2.1 Definition and significance of renewable energy:

2.1.1 What is Renewable Energy?

The notion of renewable energy has achieved broad acceptance within both policy and scholarly circles, exhibiting a notable degree of definitional convergence that is somewhat rare in the context of contemporary grand challenges. According to the International Energy Agency (IEA), renewable energy is defined as "energy derived from natural processes that are replenished at a faster rate than they are consumed." This encompasses solar, wind, geothermal, hydropower, and biomass energy sources. The European Union, in a similar vein, includes wind, solar, hydro, tidal, geothermal, biofuels, and renewable waste within its categorization of renewable energy. The United Nations Environment Programme (UNEP) also aligns with this conceptualization.

Such consistency across authoritative definitions is relatively unusual, particularly when compared to other contested notions in the environmental and policy arenas. Concepts such as sustainability, cleantech, and corporate social responsibility have attracted substantial scholarly attention, yet they continue to provoke debate and resist convergence towards universally accepted definitions. In this regard, it can be posited that renewable energy has evolved into a foundational concept within the domains of energy policy and climate change mitigation. Its definitional clarity has facilitated the development of coherent policy frameworks and has served to shape the underlying logics that drive these fields [3].

2.1.2 Importance in Sustainable Development:

There is no doubt that the importance of renewable energy to sustainable development is unparalleled. As societies strive to balance economic growth, environmental protection, and social justice, investments in renewable energy play a pivotal role in achieving these interconnected goals. Among the key contributions of renewable energy are:

1. Investments in renewable energy sources align well with the fundamental principles of sustainable development, fostering an integrated approach that balances environmental, economic, and social considerations[4].
2. Nevertheless, prevailing economic conditions and entrenched reliance on traditional energy-generation models may hinder the rapid deployment of renewable energy technologies, thereby constraining the pace of transition towards more sustainable energy systems [4].
3. Moreover, investments in renewable energy sources are inherently aligned with the objectives of environmental protection, given their potential to significantly reduce air, soil, and surface water pollution, as well as their capacity to mitigate the greenhouse effect [4].
4. It is imperative to further promote societal understanding of the local benefits derived from the use of renewable energy sources, coupled with the adoption of innovative, rapidly developing technologies that enhance the effectiveness of renewable energy systems [4].
5. Additionally, investments in renewable energy contribute to increased energy self-sufficiency and independence, particularly in rural areas that are more susceptible to energy supply disruptions, thereby reinforcing local resilience [4].

2.2 Global trends and environmental impacts:

2.2.1 Growth in global investments in renewable energy:

Global energy investment surpassed USD 3 trillion in 2024, with approximately USD 2 trillion allocated to clean energy technologies and infrastructure. This significant growth, particularly since 2020, saw spending on renewable energy, grids, and storage surpass total investments in oil, gas, and coal. According to the World Energy Investment report, however, this shift was accompanied by notable imbalances in energy investment flows, particularly regarding insufficient clean energy investments in emerging markets and developing economies (EMDE), excluding China. Despite these challenges, there were emerging signs of recovery, with clean energy investments reaching approximately USD 320 billion in 2024, marking an increase of over 50% since 2020.

In the power sector, investments in solar photovoltaic technology exceeded USD 500 billion in 2024, outpacing investments in all other generation sources combined. The ratio of clean power to unabated fossil fuel power investments reached 10:1, underscoring the urgent need for complementary investments in flexibility and storage capacity. Nuclear power investments also saw a resurgence, with total spending reaching USD 80 billion, nearly double the 2018 level. Grids, a critical bottleneck for energy transitions, saw increased investments, with expected spending of USD 400 billion in 2024. Similarly, while investments in battery storage grew, spending remained highly concentrated. In terms of energy efficiency and electrification within buildings and industry, resilience was observed, yet much of the dynamism in end-use sectors was driven by the transportation sector, particularly through robust sales of electric vehicles[5].

The trends in global investment in clean energy and fossil fuels from 2015 to 2024 are illustrated in Figure 1.1, which highlights the stark contrast between the growing investments in clean energy and the relatively stagnant or declining investments in fossil fuels over the same period. This visual representation underscores the shift towards renewable energy sources, reflecting the increasing global commitment to sustainability, while fossil fuel investments have shown limited growth or a downward trajectory in comparison.

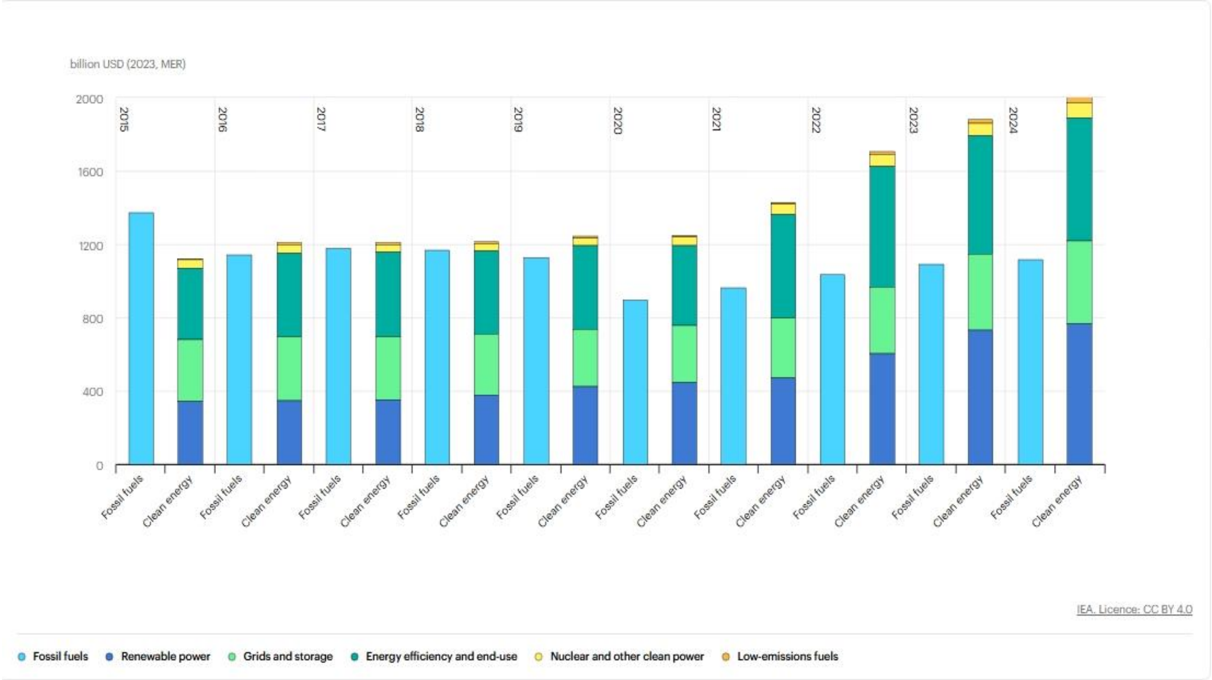

Figure 1.1: Global investment in clean energy and fossil fuels, 2015-2024 [5]

Additionally, Figure 1.2 presents global annual investments in solar photovoltaic (PV) and other generation technologies from 2021 to 2024, emphasizing the significant growth in solar PV investments, which continue to outpace other generation technologies, reinforcing the dominance of solar energy in the global energy transition.

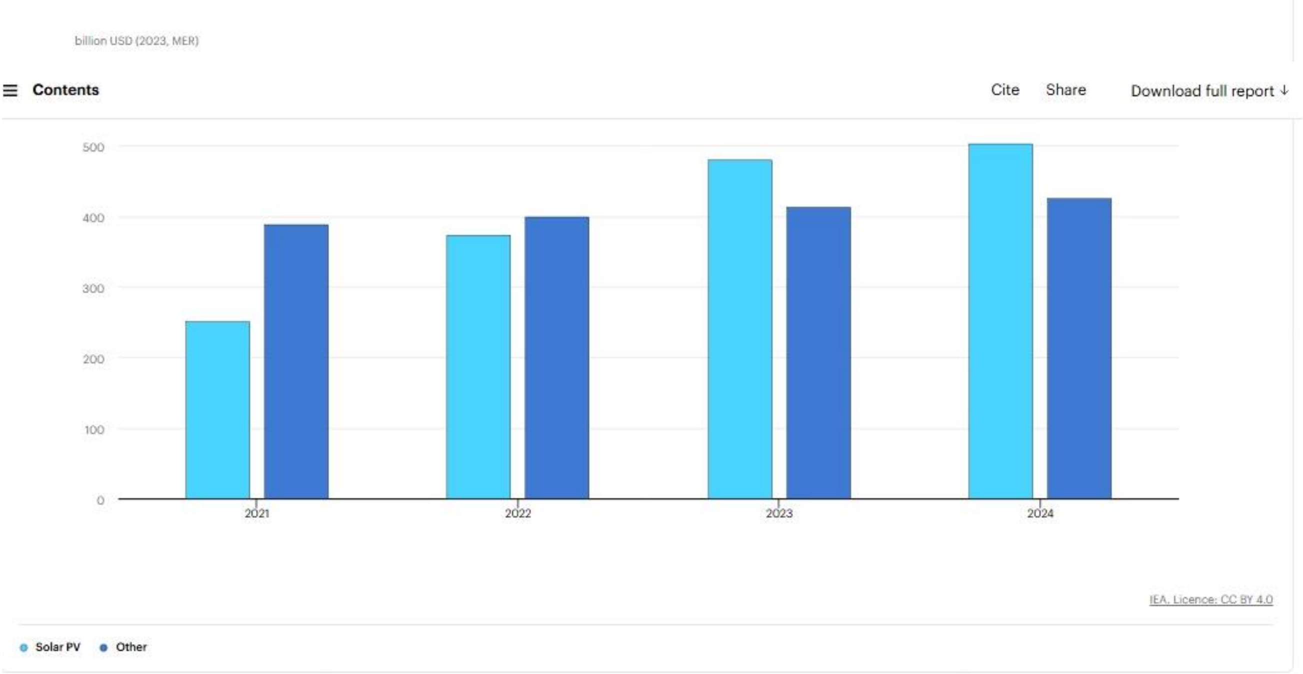

Figure 1.2: Global annual investment in solar PV and other generation technologies, 2021-2024 [5]

2.2.2 The Impact of Renewable Energy on Reducing Carbon Emissions:

The deployment of renewable energy plays a crucial role in significantly reducing carbon dioxide emissions, which are a major contributor to global climate change. As such, it is imperative to rationalize the use of fossil fuels and non-renewable energy sources within energy consumption patterns, while prioritizing the integration of renewable energy technologies to curb carbon emissions. In this context, further investment is essential to expand renewable energy capacities, particularly through the promotion of solar and wind energy. Additionally, providing incentives and support for the adoption of energy-efficient technologies and devices is critical. To achieve these goals, a comprehensive and effective energy policy must be developed and implemented, guiding the transition towards a sustainable and low-carbon energy future[6].

2.3 Challenges in renewable energy adoption:

While the adoption of renewable energy sources has been growing in many regions, widespread implementation remains constrained by a variety of political, regulatory, technological, social, and financial challenges. Fossil fuels and nuclear energy continue to receive substantial subsidies, which often outweigh the financial incentives available for renewable energy. Additionally, market failures—stemming from unfavorable financial, institutional, and regulatory environments—necessitate state intervention to facilitate the development of renewable energy infrastructures. Such interventions are crucial for building human and institutional capacity, establishing research and development frameworks, and fostering an investment-friendly environment in many countries.

A major barrier to the adoption of renewable energy is the lack of a supportive political framework, which, when absent, can undermine the feasibility of renewable energy projects despite the availability of abundant resources and favorable technological advancements. Addressing these challenges requires a systematic approach to research, aimed at enhancing the understanding of the barriers to renewable energy adoption and distribution across different national contexts. The specific obstacles faced by a country will vary depending on its unique circumstances, the dynamics of the global system, and the processes related to the flow of information and resources.

Effectively responding to these challenges is a particularly complex task, as it involves addressing global, multi-generational issues while meeting the simultaneous demands for access to critical energy services, economic and social development, and environmental sustainability [7].

3. Solar Energy as a Sustainable Resource:

3.1 Principles of solar energy conversion:

3.1.1 The Photovoltaic effect in solar cells:

The photovoltaic effect is a process through which light is converted into electricity. First observed in 1839 by Henri Becquerel, this phenomenon occurred when he immersed a platinum sheet, coated with a thin layer of silver chloride, in an electrolytic solution and illuminated the sheet while it was connected to a counter electrode. In photovoltaic (PV) technology, direct current (DC) electrical power, measured in watts (W) or kilowatts (kW), is generated when semiconductor materials absorb photons during the illumination process.

Functionally, individual PV elements, commonly referred to as solar cells, consist of a p-n junction in a semiconductor material where light absorption takes place. Unlike batteries, solar cells do not require recharging to produce electricity; once the light is cast on a solar cell, electric power generation continues. When the illumination is interrupted, however, electricity generation ceases as well. A solar cell is essentially a semiconductor diode that efficiently harnesses photonic energy from the sun to generate electrical energy. Its key physical principles involve sunlight striking the top surface, a metallic grid providing electrical contact, and an antireflective layer to improve light transmission. The junction is formed by the n-type and p-type semiconductors, with an additional metallic layer on the back surface to complete the system[8]. Figure 1.3 illustrates the photovoltaic effect in a solar cell, visually depicting how light is converted into electrical energy through the interactions at the semiconductor junction

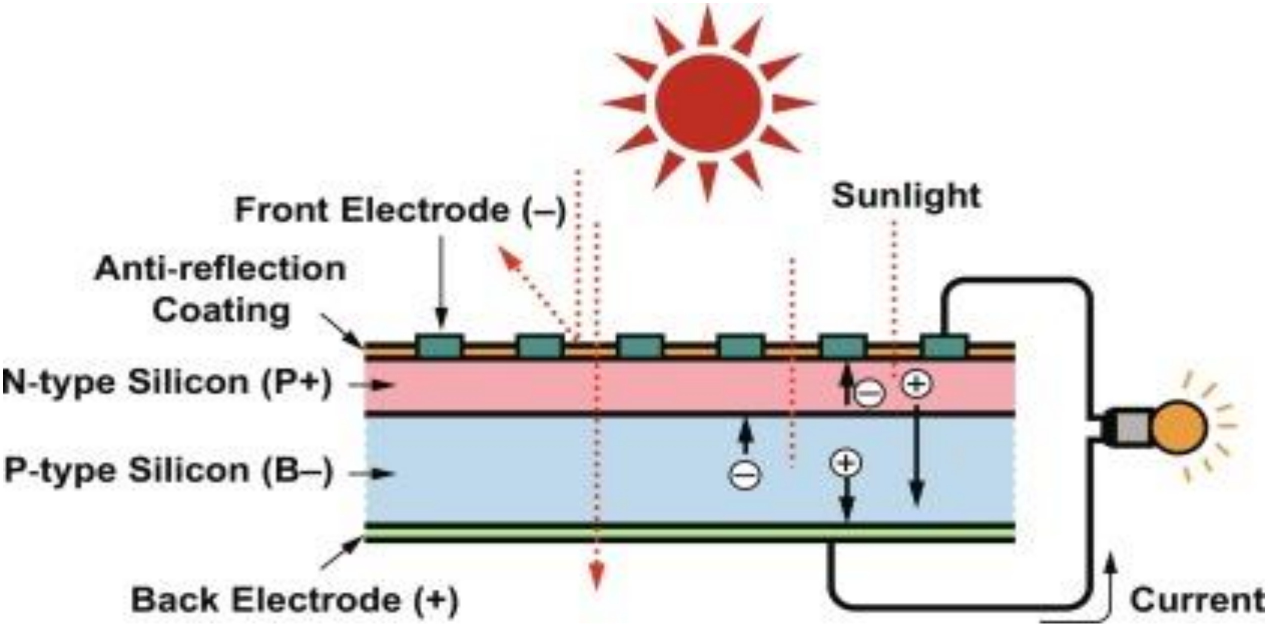

Figure 1.3: Photovoltaic effect in a solar cell[8].

3.1.2 Solar Thermal Conversion:

Solar thermal conversion is based on well-established principles of heat transport. In all thermal conversion processes, solar radiation is absorbed at the surface of a receiver, which is either in contact with or includes flow channels through which a working fluid circulates. As the receiver heats up, heat is transferred to the working fluid, which may be air, water, oil, or molten salt. The maximum temperature achievable in solar thermal conversion depends on several factors, including the level of insolation, the degree of sunlight concentration, and the measures implemented to minimize heat losses from the working fluid.

The temperature of the working fluid can be regulated through adjustments in circulation velocity, thereby aligning solar energy generation with load requirements in terms of both quantity and temperature. This flexibility enables the design of conversion systems optimized in accordance with the first and second laws of thermodynamics, ensuring both efficient energy conversion and effective temperature control [9].

Figure 1.4 illustrates the Solar Thermal Power Plant Cycle, highlighting the processes involved in converting solar energy into thermal power

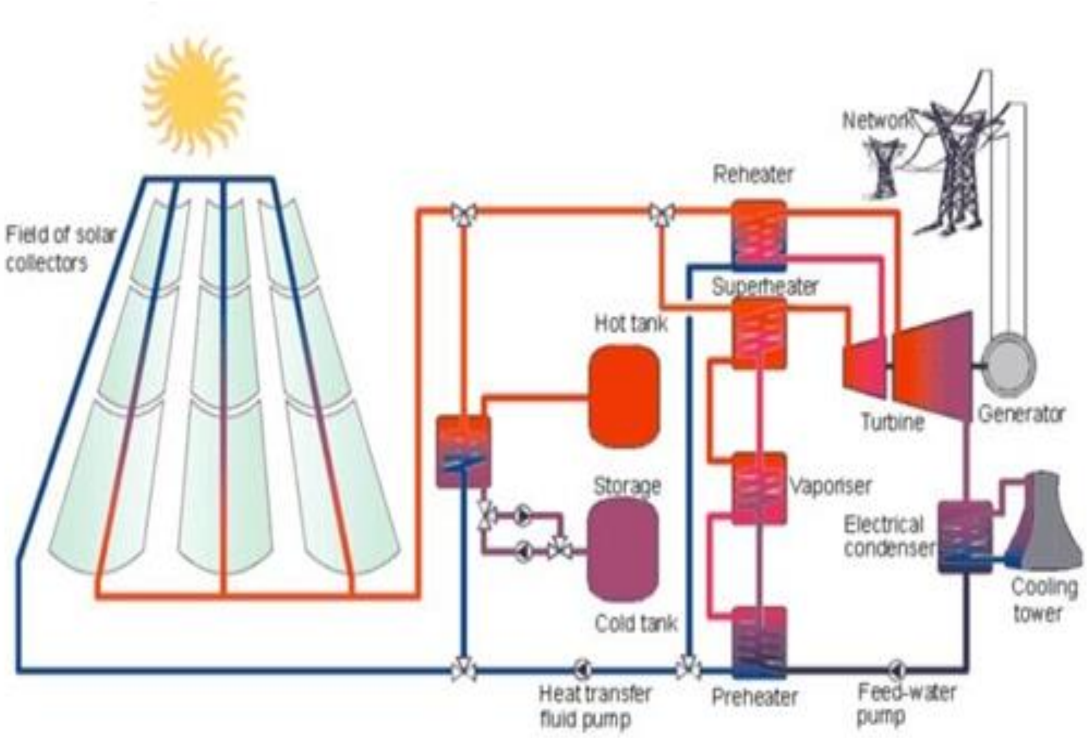

Figure 1.4: Solar Thermal Power Plant Cycle[10].

3.2 Technologies for harnessing solar power (PV, CSP):

3.2.1 Photovoltaic (PV) Systems and Panels:

Solar energy is converted into electricity in a solar cell, which generates specific electrical power. To make solar electricity usable for practical applications, multiple solar cells are interconnected to form a solar panel or photovoltaic (PV) module. For large-scale generation, these solar panels are arranged in arrays, which collectively harness greater power. Solar modules serve as the primary power generators, while batteries are required for energy storage during periods of low sunlight, such as at night or during inclement weather. Charge regulators are employed to condition the direct current (DC) output, ensuring a stable and efficient power supply. For alternating current (AC) applications, DC/AC inverters are used to convert the energy. The electrical load refers to the household appliances and devices powered by the PV solar system. Figure 1.5 illustrates the components of a photovoltaic system, providing a visual representation of the key elements involved in PV energy conversion and storage [11].

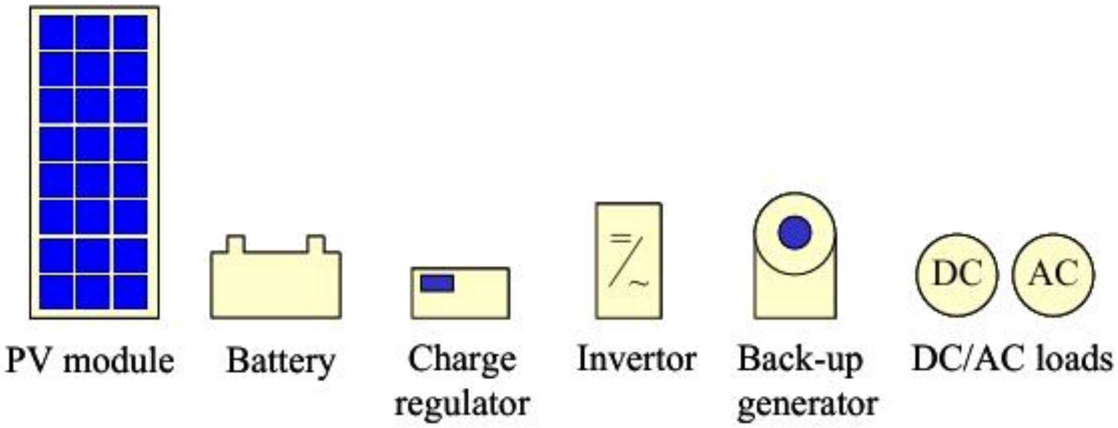

Figure 1.5: The components of a PV system[11].

3.2.1.1 Components of a PV system:

A photovoltaic (PV) solar system is composed of three main components:

1. **PV Modules or Solar Arrays**: These are the fundamental power-generating units of the system, where solar energy is captured and converted into electrical power.
2. **Balance of System (BOS)**: This includes the supporting components that ensure the system operates efficiently. The key elements of the BOS are:
   - **Mounting Structures**: These are used to secure the PV modules or solar arrays in place.
   - **Energy Storage**: Typically provided by batteries, energy storage systems are crucial for storing excess energy for use during periods of low sunlight.
   - **Lead-Acid Batteries**: A commonly used type of energy storage battery in PV systems.

  - **Nickel-Cadmium Batteries**: Another type of battery used for energy storage, offering longer lifespan and higher discharge efficiency.
  - **Charge Regulators**: These devices regulate the flow of electricity from the PV modules to prevent overcharging of the batteries.
  - **Inverters**: Inverters convert the direct current (DC) generated by the solar modules into alternating current (AC) for use by household appliances.

3. **Electrical Load**: This refers to the household appliances and devices that are powered by the electrical energy generated by the PV system.

3.2.1.2 Types of PV systems:

Photovoltaic (PV) systems can vary significantly in complexity, ranging from simple configurations to more sophisticated setups. In their simplest form, a PV system may consist of just a single PV module and an electrical load, such as in the direct powering of a water pump motor. These basic systems typically only require operation when sunlight is available. In contrast, more complex PV systems, such as those used to power a house, must operate continuously, both day and night. These systems may need to support both alternating current (AC) and direct current (DC) loads, include energy storage for reserve power, and may even incorporate a backup generator to ensure reliable operation.

Based on their configuration and functionality, PV systems are generally categorized into three main types [11]:

1. **Stand-alone Systems**: These are independent systems that are not connected to the electrical grid. They typically include solar panels, a battery storage system, and a load, making them suitable for remote areas where grid connection is unavailable.

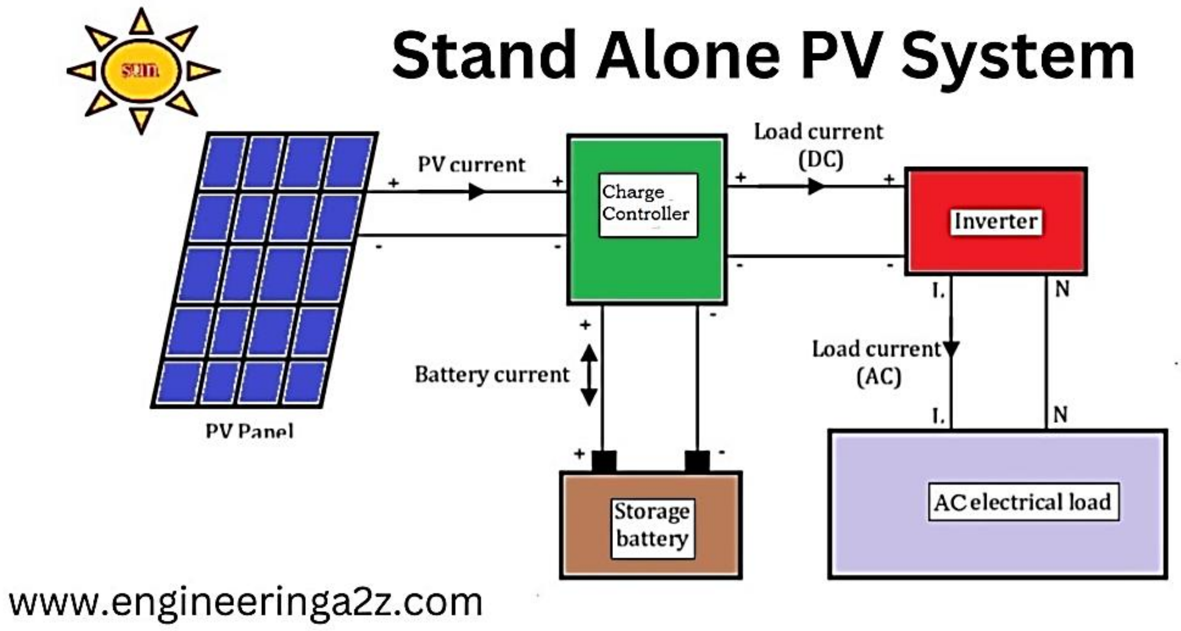

Figure 1.6: Stand-alone Systems

2. **Grid-connected Systems**: These systems are connected to the utility grid, allowing for the exchange of electricity between the PV system and the grid. Excess energy generated by the PV system can be fed back into the grid, while energy can be drawn from the grid when the solar power is insufficient.

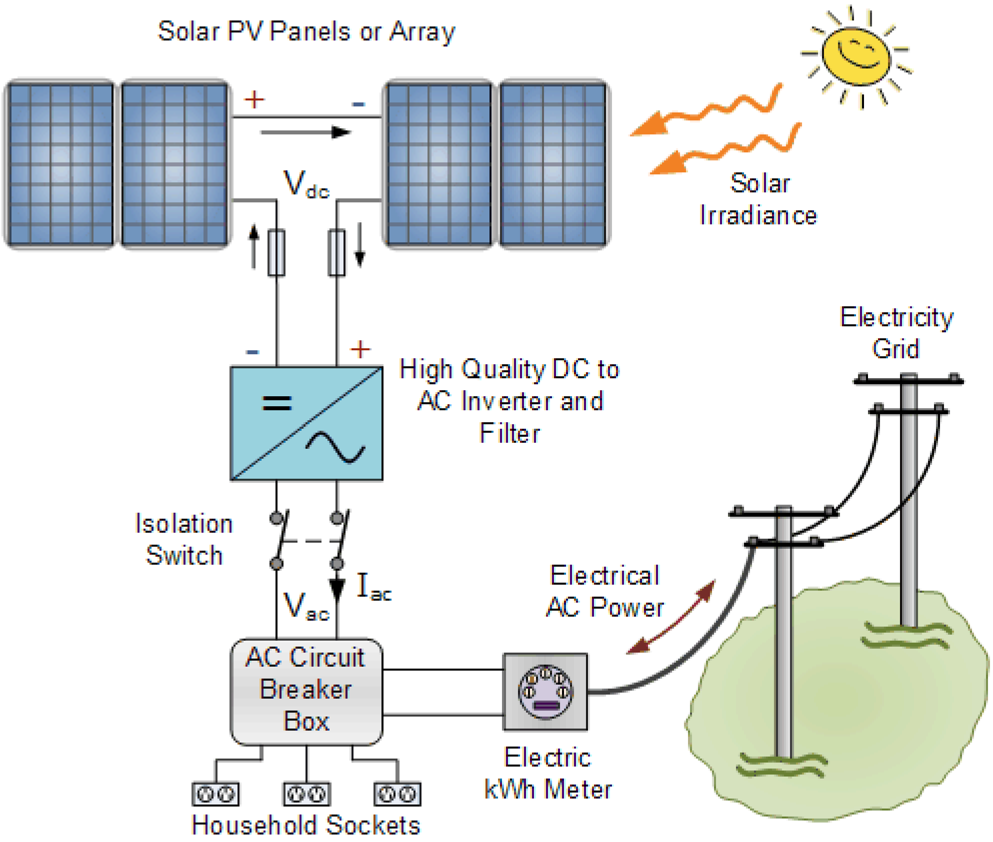

Figure 1.7 : Grid-connected Systems

3. **Hybrid Systems**: Hybrid systems combine both stand-alone and grid-connected features. They typically include energy storage, backup generators, and a grid connection, offering greater flexibility and reliability by ensuring continuous power supply under various conditions.

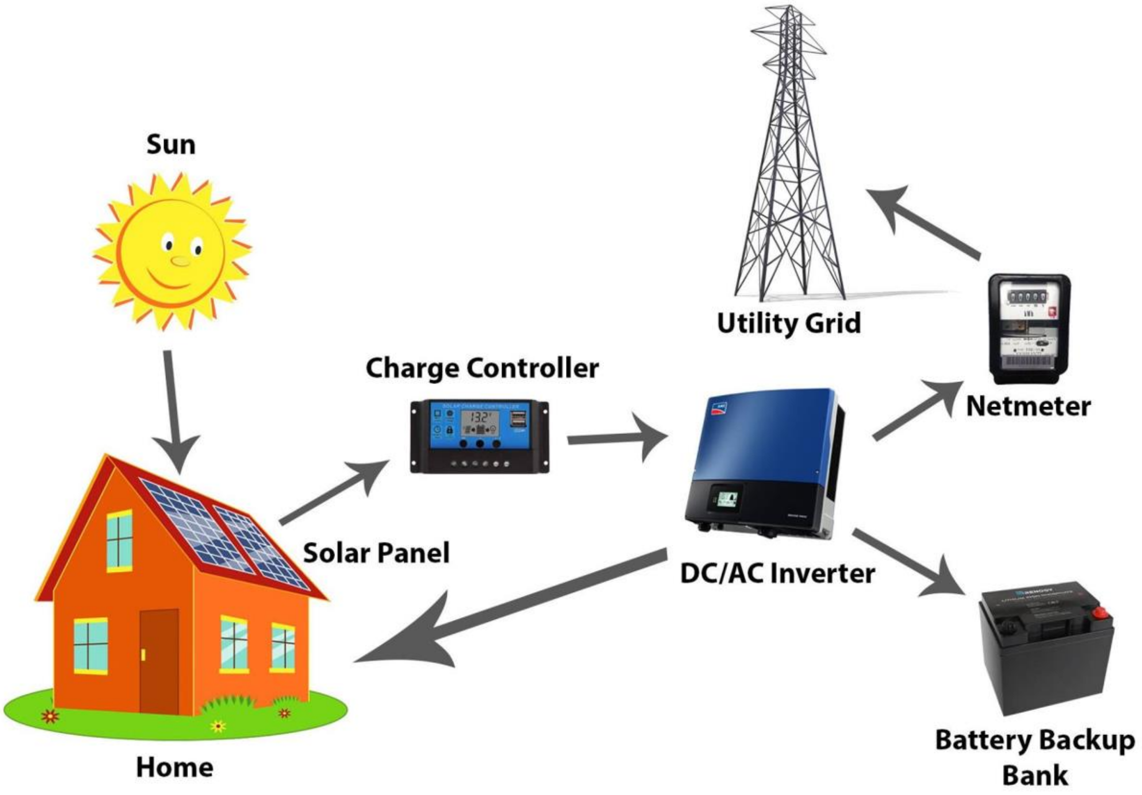

Figure 1.8: Hybrid Systems

3.2.2 Concentrated Solar Power (CSP) Systems:

Concentrated Solar Power (CSP) generates energy by focusing the heat produced by sunlight onto a limited area. Sunlight is reflected by mirrors toward a receiver, where it is absorbed by a thermal energy carrier, which forms the primary circuit. This heat is then used to drive a turbine and generate electricity, either directly (in the case of water/steam) or indirectly (via a secondary circuit). CSP holds particular promise in areas with high direct normal irradiance (DNI), such as densely populated regions. According to the current technology roadmap, CSP has the potential to become a competitive source of large-scale electricity for peak and medium loads in the sunniest regions by 2020. Furthermore, it is expected that CSP could provide baseload power between 2025 and 2030 [12].

Currently, there are four available CSP technologies: parabolic trough collector (PTC), solar power tower (SPT), linear Fresnel reflector (LFR), and parabolic dish systems (PDS). These technologies differ in their design and method of concentrating solar energy, each with its unique advantages and potential for large-scale energy production.

Figure 1.6 illustrates the currently available CSP technologies: (a) Solar Power Tower (SPT), (b) Parabolic Trough Collector (PTC), (c) Linear Fresnel Reflector (LFR), and (d) Parabolic Dish Collector (PDC) [12].

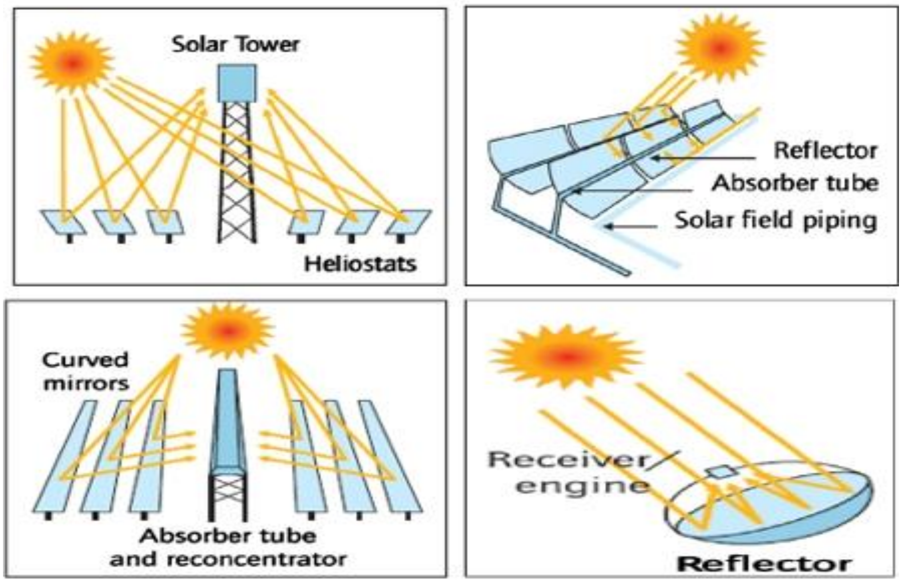

Figure 1.9: Currently available CSP Technologies:(a) STP; (b)PTC; (c) LFR; (d) PDC [12].

3.3 Advantages and limitations of solar energy:

Solar energy is increasingly recognized as a vital renewable resource, playing a key role in the global energy transition. However, it comes with both significant advantages and limitations. The following points outline the main advantages and limitations associated with the adoption of solar energy.

a) Advantages:

1. Solar energy is a clean and renewable energy source, meaning it does not produce greenhouse gases or other pollutants, contributing to the reduction of environmental harm [13].
2. It can be utilized to generate electricity in remote areas where access to grid electricity is unavailable, offering a reliable power solution in off-grid locations [13].
3. Solar energy systems require minimal maintenance and have a long operational lifespan, making them a durable and cost-effective investment over time [13].
4. They can reduce electricity costs for homeowners, and in some cases, owners can earn revenue through net metering programs, such as Solar Renewable Energy Credits (SRECs), by selling excess energy back to the grid [13].

5. Solar power can be seamlessly integrated into building design, for example, by incorporating rooftop solar panels, which helps reduce the environmental impact of buildings [13].
6. It is considered safer than conventional electricity, with fewer risks associated with energy production and distribution [13].

b) limitations:

1. Solar energy production is highly dependent on weather conditions, and cloudy or rainy days can significantly reduce the efficiency of solar panels, limiting energy output [13].
2. The initial cost of installing solar panels remains relatively high, which may deter individuals or businesses from adopting this technology [13].
3. Large-scale solar farms require significant areas of land, potentially leading to negative impacts on the surrounding ecosystems and land use [13].
4. The production of solar photovoltaics involves the use of various hazardous and toxic chemicals, some of which may have indirect environmental consequences [13].

4.Solar Energy in Algeria

4.1 Solar Potential and National Energy Policies in Algeria

4.1.1 Solar potential

Solar potential is the total amount of solar radiation energy (kWh) received on a given surface area (m²) during a given time (year) in specific location. On Fig. 1 .10, we can notice that the available energy in a year is sufficient to cover all the energetic needs of the world during the same period [14].

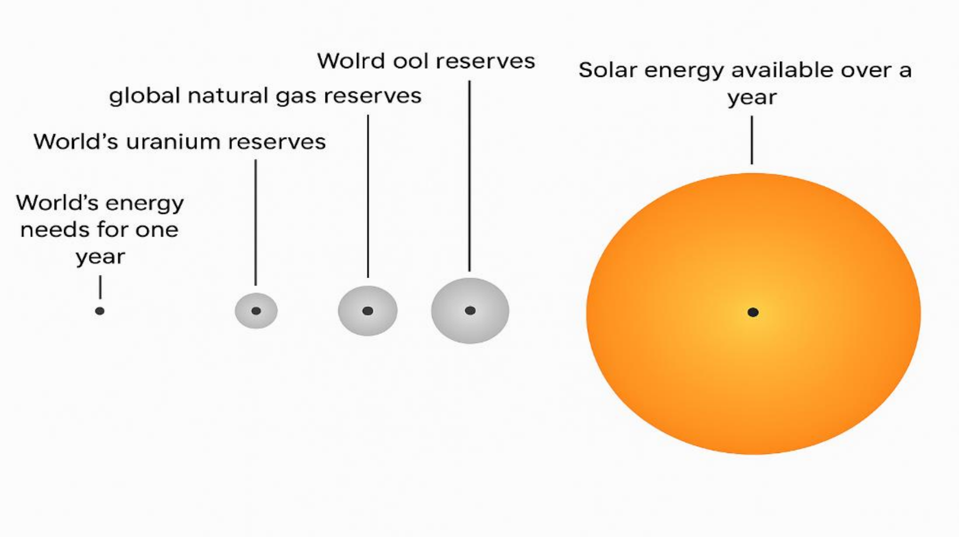

Figure 1.10: Solar energy vs. other energy sources [14].

Algeria receives an average of 3000 hours/year of solar radiation; it has the most important solar potential of the Mediterranean basin (169440 TWh/year). The average of the received solar energy in coastal regions is 1700 kWh/m²/year while it is 1900 kWh/m²/year on highlands and 2650 kWh/m²/year in the Sahara (see table 1.1). It has been proved that alone, the solar potential of the Sahara could cover all the needs of energy in the world if we put the necessary amount of investments in this field [14].

Table 1.1: Solar potential of Algeria [14].

Region	Coastal regions	Highlands	Sahara
Surface %	4	10	86
Average sunshine duration (hours/year)	2650	3000	3500
Average energy (kWh/m²/year)	1700	1900	2650

4.1.2 Algeria National Planning:

Algeria is a developing country whose economy is based mainly on the income from oil and hydrocarbons. In order to face climate change, the Algerian government has established the objective of installing 5GW of new generation facilities by 2030, which could include wind power among other things[15].

Table 1.2. Stages and targets for renewable energy production in Algeria[15].

	2015-2020 (MW)	**2020-2030 (MW)**	**Total (MW)**	**Total (%)**
Photovoltaic (PV)	3,000	10,575	13,575	61.70
Wind power	1,010	4,000	5,010	22.77
Concentrated solar power (CSP)	-	2,000	2,000	9.09
Biomass	360	640	1,000	4.55
Cogeneration	150	250	400	1.82
Geothermal	5	10	15	0.07
Total	**4,525**	**17,475**	**22,000**	

4.2 Major Solar Projects and Infrastructure Development:

4.2.1 Major Projects and Initiatives:

Algeria has significant solar potential, with an average annual solar irradiation of 2,650 kWh/m² in the Sahara. Major solar energy projects include:

- Hassi R’Mel Hybrid Power Plant (2011): Algeria’s first hybrid (solar-gas) power plant with a 25 MW solar component.
- Algeria’s PV Solar Program (2015–2030): Aims to install 13.6 GW of solar power by 2030.
- Solar 1000 MW Project (2023–2027): Launched in 2023 to develop large-scale photovoltaic (PV) farms across several regions.[16]

4.2.2 Current Challenges:

Despite ambitious targets, Algeria’s solar energy development faces:

- Slow Implementation: Delays in project execution due to administrative bottlenecks.
- Investment Barriers: Limited private sector participation due to unclear regulations.
- Grid Integration Issues: Weak electricity grid infrastructure for large-scale solar expansion.[16]

4.3 Economic and environmental benefits:

Economic benefits:

The economical benefits of the application of solar energy are as follows:

- Helps to expand production dates.
- Provides constant and excellent lighting at a minimum cost compared to other energy generators or power usage of.
- Solar energy helps improve direct and indirect employment opportunities.
- Solar energy helps to maintain foreign exchange. This is because some of the profits of the were saved from exports, otherwise spent on importing various spare portions of the electricity generator.
- Furthermore, money saved in this way can be used in other sectors such as
- health and education, which require attention.
- Despite the challenges of the power shortage, sometimes micro companies still survived. Therefore, the use of solar energy will promote the growth and development of the country's micro-development[17].

Environmental Benefits:

- It does not emit any carbon dioxide (CO_2) gasses, This prevents greenhouse effect.
- nitrogen oxide (NO) and sulfur dioxide (SO_2) are not produced at all, helping to reduce acid rain.
- Reducing carbon emissions[17].

6. Conclusion:

In this chapter, we have explored the advantages of renewable energy, with particular emphasis on solar energy as a highly promising alternative in regions characterized by abundant sunlight. The discussion encompassed the fundamental principles underlying solar energy, the various types of solar systems, as well as the environmental and economic benefits associated with their deployment.

This introduction serves as a foundation for a deeper understanding of the technical challenges involved in accurately assessing solar energy potential, a subject that will be further elaborated upon in the forthcoming chapters. The next section will delve into predictive models, with a focus on the Support Vector Regression (SVR) model, and the enhancement of its performance through the integration of the Particle Swarm Optimization (PSO) algorithm.

Chapter 2

Support Vector Regression and Particle Swarm Optimization

1. Introduction:

In recent years, effective prediction and modeling have emerged as essential tasks in a wide range of scientific and industrial domains, including renewable energy, finance, and healthcare. Within the diverse landscape of machine learning techniques, Support Vector Regression (SVR) has garnered significant interest due to its capacity to manage nonlinear regression problems. SVR extends the Support Vector Machine (SVM) framework to regression tasks, thereby offering a flexible approach to modeling complex relationships. Nevertheless, the performance of SVR is highly contingent on the appropriate selection of its hyperparameters—namely, the penalty parameter CCC, the epsilon-tube ε\varepsilonε, and the kernel parameter γ\gammaγ. The process of tuning these parameters remains challenging, as suboptimal choices can substantially compromise the model's predictive accuracy.

To mitigate this challenge, recent studies have turned to Particle Swarm Optimization (PSO) as a means of enhancing SVR's performance. Initially introduced by Kennedy and Eberhart (1995), PSO belongs to the broader family of evolutionary computation techniques. As an optimization algorithm, PSO is well-suited to address complex optimization tasks by simulating the collective behavior of social organisms, such as bird flocks or fish schools. Its ability to navigate multidimensional search spaces efficiently has made it a popular choice for hyperparameter tuning in machine learning contexts. Indeed, integrating PSO into SVR parameter selection processes has shown promise in improving forecasting accuracy across various applications [18].

2. Support Vector Regression (SVR):

2.1 Fundamentals of Regression Analysis

2.1.1 Linear Regression Models

Simple (two-variable) regression and multiple regression are complementary subsets of the basic single-equation linear regression model, which can be represented as [19]

$$Y = a + \sum_{i=1}^{k} bi\, Xi + u \tag{2.1}$$

2.1.1.1 Simple Linear Regression

Simple linear regression lives up to its name: it is a very straightforward, simple linear approach for predicting a quantitative response Y on the basis of a single predictor variable X. It assumes that there is approximately a linear relationship between X and Y. Mathematically, we can write this linear relationship as[20] :

$$Y \approx \beta_0 + \beta_1 X \tag{2.2}$$

2.1.1.2 Multiple Linear Regression

Multiple linear regression is an extension of simple linear regression that takes into account more than one explanatory variable. In both circumstances, we continue to use the term 'linear' since we believe the response variable is closely related to a linear combination of the explanatory variables.

The equation for multiple linear regression has the same form as that for simple linear regression but has more terms:

$$Y_i = \beta_0 + \beta_1 x_{1i} + \beta_2 x_{2i} + \cdots + \beta_p x_{pi} + e_i \quad (2.3)$$

As for the simple case, β0 is the constant – which will be the predicted value of y when all explanatory variables are 0. In a model with p explanatory variables, each explanatory variable has its own β_coefficient [21].

2.1.2 Nonlinear Regression Approaches

The fundamental concept of nonlinear regression is identical to that of linear regression, which is to establish a relationship between a response Y and a vector of predictor variables **x** = $(x_1,\ldots\ldots,x_k)^T$. Nonlinear regression often occurs when there are physical grounds for thinking that the connection between the response and the predictors follows a certain functional shape, whereas linear regression is frequently employed to create a completely empirical model. A nonlinear regression model has the form

$$Y_i = f(x_i, \theta) + \varepsilon_i, i = 1, \ldots, n \quad (2.4)$$

where the Yi are responses, f is a known function of the covariate vector $x_i = (x_{i1},\ldots\ldots,x_{ik})^T$ and the parameter vector $\theta = (\theta_1,\ldots,\theta_p)^T$, and ε_i are random errors. The ε_i are usually assumed to be uncorrelated with mean zero and constant variance [22].

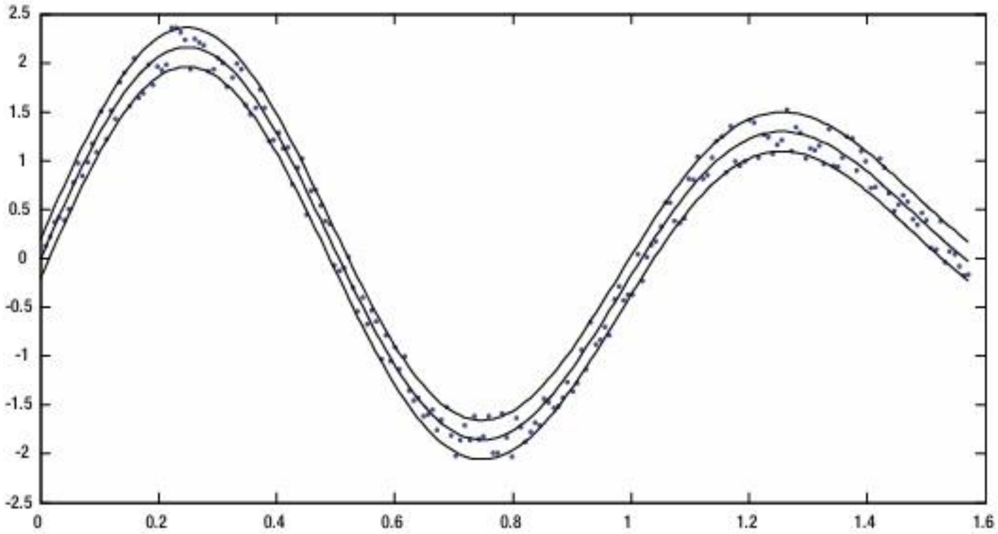

Figure 2.1: Nonlinear regression[23]

2.1.3 Advanced Regression Techniques

2.1.3.1 Decision Tree Regression:

Decision Trees (DT) represent a class of supervised learning models that are non-parametric and well-suited for both regression and classification tasks. Fundamentally, a decision tree is constructed by recursively partitioning the dataset into increasingly homogeneous subgroups through a series of binary splits. This recursive partitioning yields a hierarchical tree structure in which leaf nodes correspond to the final predicted outcomes. The term *tree-based regression* derives from this hierarchical organization, which facilitates the prediction process by evaluating data along successive splits.

A typical decision tree comprises three distinct types of nodes:

- **The root node**, which initiates the partitioning process and represents the first decision point in the tree.
- **Interior nodes**, which embody the decision criteria or model attributes, guiding the branching at each level.
- **Leaf nodes**, also known as terminal nodes, which provide the final prediction or classification once all relevant splits have been performed.

2.3.1.2 Random Forest Regression:

Random forest a decision tree-based ensemble approach, is widely employed in remote sensing investigations. Non-parametric prediction models, known as decision trees, use a multistage decision method. Classification and regression trees can predict discrete and continuous output variables. The tree structure includes a root node, internal nodes (splits), and terminal nodes (leaves) [24].

2.2 Support Vector Regression (SVR) Theory:

2.2.1 Difference Between Classification and Regression in SVM (SVM vs SVR)

2.2.1.1 SVM for Classification:

The classification problem can be restricted to consideration of the two class problem without loss of generality. In this problem the goal is to separate the two classes by a function which is induced from available examples. The goal is to produce a classifier which will work well on unseen examples, i.e. it generalises well. Consider the example in Figure 1. Here there are many possible linear classifiers that can separate the data well, but there is only one which maximises the margin (maximises the distance between it and the nearest data point of each class). This linear classifier is termed the optimal separating hyperplane. Intuitively, we would expect this boundary to generalise well as opposed to the other possible boundaries[25].

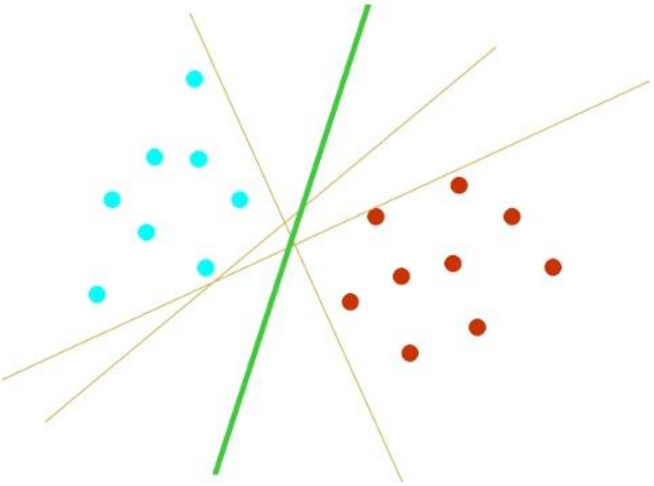

Figure 2.2: Optimal Separating Hyperplane

2.2.1.2 SVM for Regression

SVM Regression (SVR) is a technique that uses training data to predict a function that translates an input item to a real integer. SVR has characteristics with the classifying SVM, including kernel technique for non-linear mapping and margin maximization.

A training set for regression is represented as follows [26]:

$$D = \{ (X1, Y1), (X2, Y2), \ldots, (Xm, Ym) \} \tag{2.5}$$

2.2.2 Mathematical Formulation:

Support vector regression is a computational intelligence learning device that constructs the optimal hyper-plane and minimizes the sum of the distances of the training samples. A significant advantage of SVR over other computational intelligence techniques is the application of structural risk minimization (SRM) principle in its model formulation instead of empirical risk minimization for other methods. In SVR formulation, the error is described as the sum of a term (that is related to the Vapnik-Chervonenkis plane) and the trianing error set. And the years of SVR algorithm's is trying to establish input-output correlation on a group of observations from the train data set. Let us consider the training data points in (x_1, y_1),..........(x_m, y_m), with m samples and n-dimensional vector input $x_i \in R^n$, a regression function is presented in equation (1) where $\langle w \bullet x \rangle$represents dot product in R^n space.

$$F(x, w) = \langle w \bullet x \rangle + b \tag{2.6}$$

where $w \in R^n$ and b represents a bias term that can be neglected for zero mean preprocessed data [27].

- Primal Optimization Problem:

minimise $\frac{1}{2}\|w\|^2 + C\sum_{j=1}^{m} \left(\xi_j + \xi^*{}_j\right)$

$$subject\ to \qquad \left\{ \begin{array}{c} y_j - \langle w \bullet x_j \rangle - b \leq \varepsilon + \xi_j \\ \langle w \bullet x_j \rangle + b - y_j \leq \varepsilon + \xi^*{}_j \\ \xi_j\ and\ \xi^*{}_j \geq 0 \text{ for all j} = 1,2,\ldots\ldots,k \end{array} \right\}$$

(2.7)

Where:

- w is the weight vector
- b is the bias term
- ξ_i, ξ_i* are slack variables for violations above and below the ε-tube
- C > 0 is the regularization parameter
- ε is the width of the insensitivity zone

- Dual Problem Formulation:

Maximize $-\frac{1}{2}\sum_{i,j=1}(\alpha_{\text{i}} - \alpha_{\text{i}}*)(\alpha_{\text{j}} - \alpha_{\text{j}}*)\langle x_i, x_j\rangle - \varepsilon\sum_{i=1}^{1}(\alpha_{\text{i}} + \alpha_{\text{i}}*) + \sum_{i=1}^{1} y_i\,(\alpha_{\text{i}} - \alpha_{\text{i}}*)$ (2.8)

Subject to $\sum_{i=1}^{1}(\alpha_{\text{i}} - \alpha_{\text{i}}*) = 0$ and $\alpha_{\text{j}}, \alpha_{\text{j}}* \in$ [0,C]

2.2.3 ε-Insensitive Loss Function:

The use of the loss function $l(f(x), y) = max(0, |y - f(x)| - \varepsilon)$ introduces a new parameter the width of the insensitivity zone ε. By making ε a variable of the optimisation problem we have

$$l(f(x), y) = max(0, |y - f(x)| - \varepsilon) + \nu\varepsilon. \qquad (2.9)$$

The update equations must now be expressed in terms of αi, αt, and ε, which is permitted to vary throughout the optimization process. Setting $\delta t = yt - f(xt)$ the updates are $(for\ i = 1, \ldots, t - 1)$

$$(\alpha_i,\ \alpha_t, \varepsilon) = \begin{cases} (1 - \lambda\eta)\alpha_i, \eta sgn\delta t, \varepsilon + (1 - \nu)\eta) & if\ |\delta t| > \varepsilon \\ ((1 - \lambda\eta)\alpha_i, 0, \varepsilon - \eta\nu) & otherwise. \end{cases} \qquad (2.10)$$

This means that every time the prediction error exceeds ε, we increase the insensitive zone by ην. If it is smaller than ε, the insensitive zone is decreased by η(1 − ν) [28].

2.2.4 Slack Variables and Margin Tolerance:

The margin is fitting as many data points as possible within a specified margin (epsilon, ε) while minimizing the margin violation.

Margin = $\frac{1}{\|w\|}$

By minimizing $||w||^2$ to maximize the margin, the training in SVR becomes a constrained optimization problem as follows**.**

Minimize : $L(w) \; = \frac{1}{2}\|w\|^2$

Subject to: $y_i - \; w \; * \; x_i - \; b \; \leq \varepsilon$ (2.11)

$$w \; * \; x_i + \; b - y_{\,i} \leq \varepsilon$$

The solution of this problem does not allow any errors. To allow some errors to deal with noise in the training data, the soft margin SVR uses slack variablesξ andξ*.

Then, the optimization problem can be revised as follows.

Minimize : L(w, ξ) = $\frac{1}{2}\|w\|^2$ + C$\sum_i(\xi_{2i}, \xi_{2i}{}^{*})$, C > 0

Subject to:

$$yi - \; w \; * \; xi - \; b \; \leq \varepsilon \; + \; \xi i \qquad \forall (xi, yi) \; \in \; D \tag{2.12}$$

$$w \; * \; xi + \; b \; - \; yi \leq \varepsilon \; + \; \hat{\xi} i * \forall (xi, yi) \; \in \; D$$

$$\xi i \; , \xi i * \geq \; 0$$

The constant C > 0 is the trade-off parameter between the margin size and the amount of errors. The slack variables ξandξ* deal with infeasible constraints of the optimization problem by imposing the penalty to the excess deviations which are larger than ε[29].

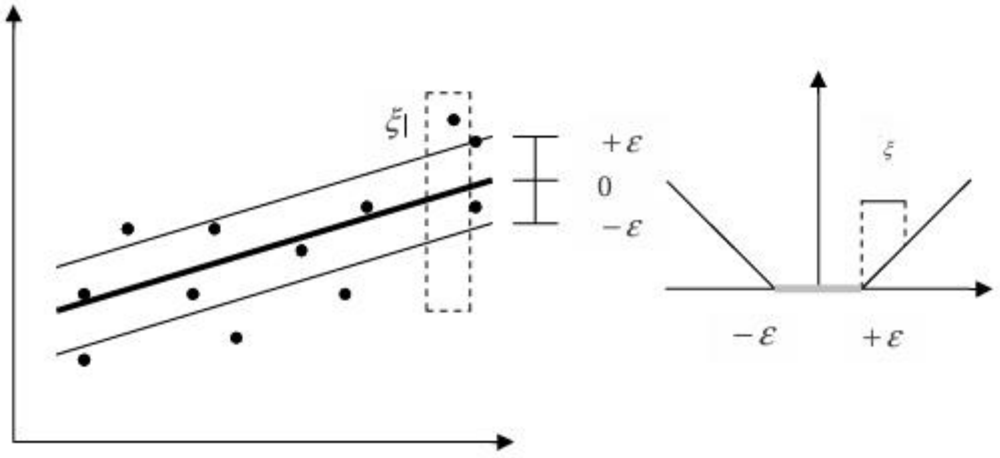

Figure 2.3: The soft margin loss setting corresponds to a linear SV machine[30]

2.3 Kernel Methods in SVR:

The function for converting a lower-dimensional data set into a higher-dimensional data set a kernel helps to find a hyper plane in a higher-dimensional space, while reducing the computational cost. The kernel function for support vector regression (SVR) is a crucial component that determines the relationship between input data and predicted output values. The choice of kernel function affects the performance and flexibility of the SVR model. Here are some kernel functions commonly used for SVR :

2.3.1 Linear Kernel Function:

The linear kernel is the simplest kernel function and works well when the relationship between input and output variables needs to be linear. It is defined as:

$$\mathrm{K}(\mathrm{x}, \mathrm{z}) = \mathrm{x}, \mathrm{z} \tag{2.13}$$

2.3.2 Radial Basis Function (RBF) Kernel:

For > 0, the Gaussian kernel is defined by

$$K(\mathrm{x} - z) = exp\left(-\frac{\|\mathrm{x} - z\|^2}{2\sigma^2}\right) \tag{2.14}$$

From the definition of the Gaussian kernel, we deduce that all points have norm 1 in the resulting feature space as (xx) = exp(0) = 1. Also, the parameter controls the flexibility of the kernel similarly to the degree d in the polynomial kernel. Small values of correspond to large values of d since they allow classifiers to fit any label, risking over fitting. In such cases, the kernel matrix becomes close to the identity matrix. On the other hand, large values gradually reduce the kernel to a constant function, making it impossible to learn any non-trivial classifier. The feature space has infinite dimension for every value of, but the weight decays very fast on the higher-order features for large values. In other words, although the rank of the kernel matrix will be full for all practical purposes, the points lie in a low-dimensional subspace of the feature space [31].

2.3.3 Polynomial Kernel:

Polynomial kernels The derived polynomial kernel for a kernel k_1 is defined as

$$k(x, z) = p(k_1(x, z)) \tag{2.15}$$

where p(.) represents any polynomial with positive coefficients.

The special case

$$k_d(x, z) = ((x, z) + R)^d \tag{2.16}$$

defined over a vector space X of dimension n, with R and d as parameters [31].

2.3.4 Kernel Selection Methodology :

Provided some random dataset, it is not defined in advance that which kernel may prove to be the best one. For a problem related to the linear separable dataset, linear kernel is acceptable. It does not make sense to employ the linear classifier when the data is not linearly separable, it is suggested to use an RBF kernel in such situation. Linear problems are resolved using the linear support vector machines while for non-linear problems, RBF kernel may be employed. The Support vector decision region corresponding to the RBF kernel is a linear decision area. Creating non-linear permutations of the features to strengthen the sample dataset and upgrade it to a corresponding feature space bearing higher dimensional attributes is the main task of an RBF kernel. In this space, a linear decision boundary may be used to separate the classes. A hyper parameter search is performed and different kernels are compared with others [32].

2.4 Hyper parameter Optimization

2.4.1 Regularization Parameter (C) :

Regularization parameter. The strength of the regularization is inversely proportional to C. Must be strictly positive. The penalty is a squared l2. For an intuitive visualization of the effects of scaling the regularization parameter C[33].

2.4.2 ε-Tube Width Optimization:

Epsilon in the epsilon-SVR model. It specifies the epsilon-tube within which no penalty is associated in the training loss function with points predicted within a distance epsilon from the actual value. Must be non-negative[33].

2.4.3 Gamma (γ) Parameter in Kernels:

the gamma parameter defines how far the influence of a single training example reaches, with low values meaning ‘far’ and high values meaning ‘close’. The gamma parameters can be seen as the inverse of the radius of influence of samples selected by the model as support vectors[33].

2.5 Advantages and Limitations of SVR:

2.5.1 Advantages of SVR:

1. SVR are known for their ability to tackle the standard problem of over-fitting, especially in multivariate settings. Their findings have indicated that both premiums to be predictable under fair levels of transaction costs and various forecasting horizons[30].

2. The SVR algorithm has acted as a filter because it has been capable to associate to each input crop an output image, which has been subsequently used to determine if the crop has contained or not a mass[30].

3. Robust SVRs are outlier-proof, which implies that they can model datasets containing outliers without altering the quality of predictions.

2.5.2 Limitations of SVR:

1. The difficulty in interpreting SVR models lies in the fact that they rely on support vectors in a higher-dimensional space.

2. Careful parameter selection: SVR performance depends on the proper selection of parameters, such as the value of the regularization parameter and the kernel function, which may require fine-grained optimization.

3. Handling missing data: SVR cannot directly handle missing data, and it is necessary to impute the missing values.

3. Particle Swarm Optimization (PSO):

3.1 Fundamentals of PSO algorithms:

3.1.1 Definition:

The Particle Swarm Optimization (PSO) algorithm constitutes a stochastic optimization technique inspired by the collective behavior observed in biological swarms. Rooted in observations of social interactions among animals—such as insects, flocks of birds, and schools of fish—PSO models how individuals within a group coordinate their movements and share information to enhance the search for resources. Each particle in the swarm continuously adjusts its search trajectory by incorporating both its own learning experience and the information gleaned from neighboring particles.

The conceptual foundation of PSO is closely related to two prominent research traditions. First, PSO draws on principles from evolutionary algorithms, adopting a population-based search strategy that enables the algorithm to explore large regions of the solution space simultaneously. Second, PSO is informed by the field of artificial life, which investigates the design of artificial systems that exhibit life-like behaviors and adaptive characteristics (see Kennedy & Eberhart, 1995; and subsequent developments in[34].

3.1.2 PSO Algorithm :

Particle Swarm Optimization (PSO) is a population-based, self-adaptive, and stochastic optimization technique. The algorithm begins by initializing a population of particles, each with an assigned velocity. For each particle, the objective function is evaluated at its current position, enabling the identification of both the best function value encountered so far (personal best) and the best position within the particle's local neighborhood (neighborhood best).

Subsequently, PSO updates each particle's velocity by considering three components: its current velocity, its personal best position, and the best position among its neighbors. The position of each particle is then updated by adding the velocity to the current position, ensuring that particles remain within the predefined search space boundaries. This iterative process of updating positions and velocities continues until a stopping criterion is met, such as a maximum number of iterations or a satisfactory convergence threshold [35].

.

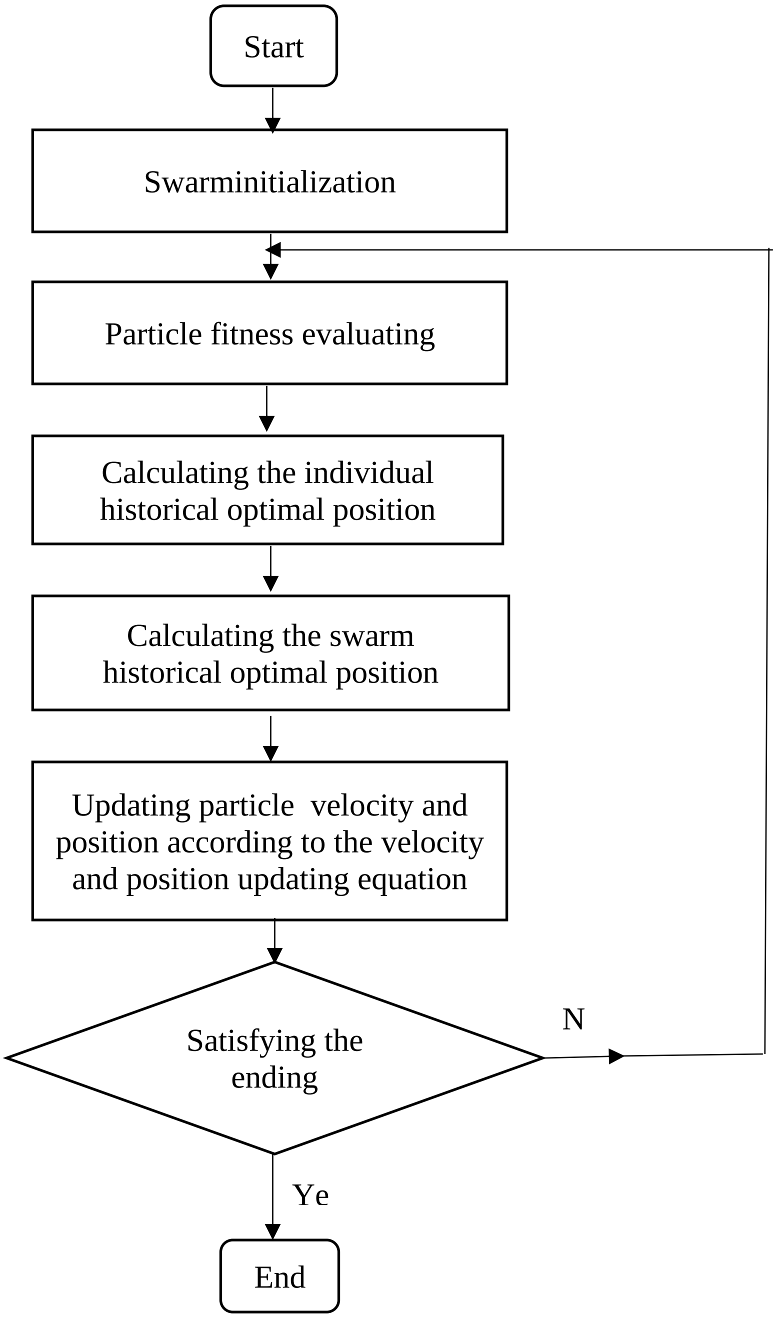

Figure 2.4: Flowchart of the particle swarm optimization algorithm[34]

3.1.3 Key Components:

3.1.3.1 Number of particles:

The number of particles allocated to solving the problem depends essentially on two parameters: the size of the search space and the ratio between the machine's computing

capacity and the maximum search time. There is no rule for determining this parameter; conducting numerous tests allows one to gain the experience necessary to understand this parameter[36].

3.1.3.2 Neighborhood Topology:

The neighborhood topology defines the neighborhood with which each particle can communicate. There are many combinations, the following being the most commonly used:

a) star topology: each particle is connected to all the others, i.e. the neighborhood optimum is

the global optimum;

b) ring topology: each particle is connected to n particles, this is the most used topology;

c) spoke topology: the particles communicate only with a single central particle [36].

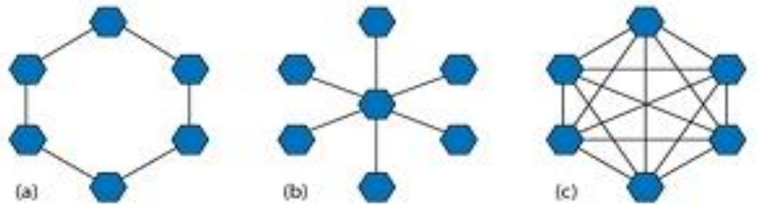

Figure 2.5: Neighborhood topologies : (a) ring , (b) spoke, (c) star[36].

3.1.3.3 Confidence Coefficients:

The confidence variables weight the particle's tendencies to follow its instinct for conservation or its panurgisme. Random variables p_1 and p_2 can be defined as follows:

$$\begin{cases} p_1 = r_1 + c_1 \\ p_2 = r_2 + c_2 \end{cases} \tag{2.17}$$

Where r_1 and r_2 follow a uniform distribution on [0..1] and c_1 and c_2 are positive constants determined empirically and according to the relation c_1+ c_2 ≤4[36].

3.1.3.4 Maximum Velocity:

Velocity can be limited by a maximum Velocity V_{max} and a minimum Velocity V_{min} to prevent particles from moving too quickly or too slowly from one region to another in the search space[36].

3.1.3.5 Inertia:

An inertia factor Φ can be applied to speed to control its influence[36].

3.1.3.6 Swarm Initialization:

The particle positions and their initial velocities must be randomly initialized according to a uniform distribution over [0 1]. However, regarding the particle positions, it is preferable to use a SOBOL sequence generator, which is more relevant for the homogeneous arrangement of particles in an n-dimensional space [36].

3.1.3.7 Stopping Criterion

The stopping criterion differs depending on the optimization problem posed and the user's constraints. It is strongly recommended to provide the algorithm with an exit gate since convergence to the global optimal solution is not guaranteed in all cases, even if experiments demonstrate the method's high performance [36].

3.1.4 Workflow:

The PSO algorithm employs a swarm of particles which traverse a multidimensional search space to seek out optima. Each particle is a potential solution and is influenced by experiences of its neighbors as well as itself. Let xi(t) be the position in the search space of the i-th particle at time step t. The initial velocity of a particle is regulated by incrementing it in the positive or negative direction contingent on the current position being less than the best position and vice-versa.

The random number generator was originally multiplied by 2 so that particles could have an overshoot across the target in the search space half of the time. These values of the constants, known as the cognition and social acceleration co-efficient were found to effect superior performance than previous versions. the PSO algorithm has undergone numerous improvements and extensions aimed at guaranteeing convergence, preserving and improving diversity as well as offsetting the inherent shortcomings by hybridizing with parallel EC paradigms [37].

3.2 Position and velocity update equations:

The particle swarm consists of n particles, and the position of each particle represents a solution in the search space. Particles change state according to the following three principles:

- Maintain inertia
- Change state based on their most optimistic position
- Change state based on the most optimistic position of the group.

The position of each particle is affected by both the most optimistic position during its movement (individual experiment) and the position of the most optimistic particle in its surroundings (global experiment). The update of the position xi(t) and velocity vi(t) of a particle pi is represented by the equations

Velocity Update:

$$V_i\ (t+1) = w \cdot v_i(t) + c_1 r_1 [xp_i(t) - x_i(t)] + c_2 r_2\ [g(t) - x_i(t)] \tag{2.18}$$

Position Update:

$$X_i(t+1) = x_i(t) + v_i(t+1) \tag{2.19}$$

Where ω is the inertia, c1 and c2 are constant coefficients set by the user, r1 and r2 are random numbers in the range [0 1], drawn at each iteration, g(t) is the best solution found up to time t, and $xp_i(t)$ is the best solution found by particle pi.

Let f(x) be the objective function to be optimized (fitness) and n be the number of particles.

The essential steps of particle swarm optimization are presented by the following algorithm:

```
1- Random initialization of the particle population and velocities.
2- Find the best fitness value f at t=0.
    3- Processing
        Repeat until the end of the iteration.
        Repeat for each particle.
        Generate the new velocity value using equation (2.18).
        Calculate the new position using equation (2.19).
        Evaluate the fitness value.
        Find the best position for each particle.
    End.
    Find the best global position.
End
```

In general, the stopping criterion can be a fixed number of iterations, a function of the objective function (fitness), or when the particle velocities tend toward 0[38].

3.3 Advantages of PSO:

PSO has some advantages over other similar optimization techniques, namely the following:

1) PSO is easier to implement and there are fewer parameters to adjust.

2) In PSO, every particle remembers its own previous best value as well as the neighborhood best; therefore, it has a more effective memory capability.

3) PSO is more efficient in maintaining the diversity of the swarm (more similar to the ideal social interaction in a community), since all the particles use the information related to the most successful particle in order to improve themselves.[39]

3.4 Applications of PSO in hyper parameter tuning:

The PSO algorithm is utilized to optimize the hyperparameters of the machine learning models. Recent studies have demonstrated that swarm intelligence, particularly PSO, is capable of achieving highly effective results in hyperparameter optimization tasks, particularly when dealing with large-scale datasets. The findings of this study also provide evidence of the efficacy of PSO in optimizing hyperparameters for improved performance[40].

4. Integration of SVR and PSO:

The procedure of SVR-PSO is briefly demonstrated as follows:

Step 1: Initialization

Begin by initializing the population of three particles, each representing the hyperparameters (σ, ε, C). Assign each particle a random initial position and velocity.

Step 2: Compute Initial Objective Values

Evaluate the initial objective function values using the current positions of the three particles. For each particle, record its local best objective value, denoted as , $f_{\text{best}i}$ corresponding to its own best position. Simultaneously, determine the global best objective value, , $f_{\text{globalbest}i}$, based on the particle exhibiting the best performance across the entire population.

Step 3: Update Inertia, Velocity, and Position

Update the inertia weight, velocity, and position of each particle. The inertia weight is commonly adjusted using a linear decreasing function, facilitating a balance between exploration and exploitation. Subsequently, recompute the objective values using the updated positions of the three particles

Step 4: Update Objective Values

For each iteration, compare the objective value at each particle's current position with its local best objective value, f_{besti}. If the current objective value is superior (i.e., exhibits a lower forecasting error), update f_{besti} accordingly. In this study, forecasting errors are measured using both the Mean Absolute Percentage Error (MAPE) and the Root Mean Square Error (RMSE). A dynamic switching mechanism between MAPE and RMSE is employed: if MAPE yields a lower error than RMSE (or vice versa), the smaller error metric is prioritized to ensure optimal objective value selection.

Step 5: Determine Best Particles

If a particle's current objective value is also better than the global best value $f_{\text{globalbest}}$, update the global best value accordingly and record the corresponding particle as the best performer in the current iteration

Step 6:

Check whether the stopping criterion (based on forecasting error thresholds) has been satisfied. If so, the final $f_{\text{globalbest}i}$ is designated as the solution. Otherwise, repeat the process starting from Step 3.

The detailed procedure of the SVR-PSO algorithm is illustrated in Figure 2.6 [41]

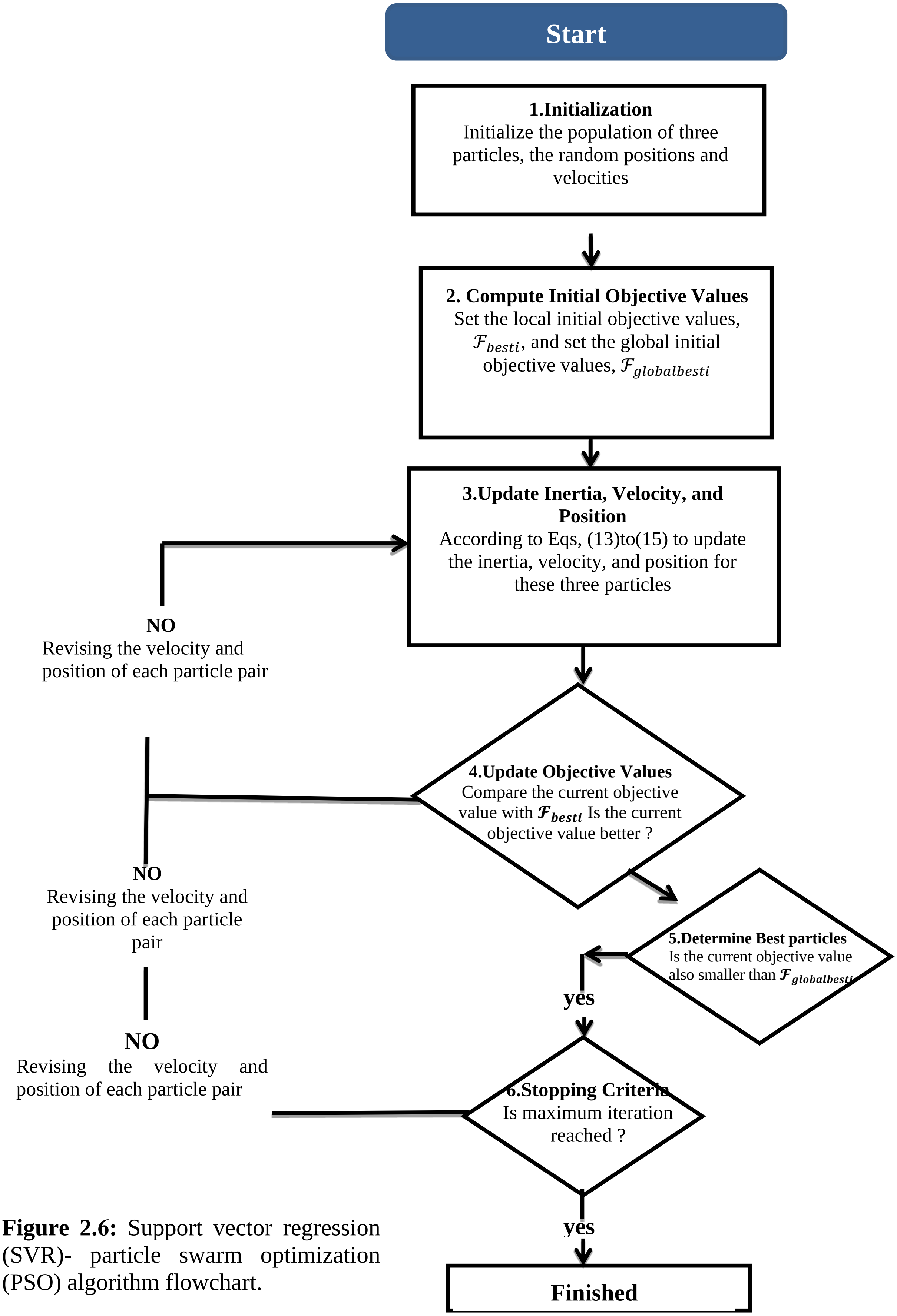

Figure 2.6: Support vector regression (SVR)- particle swarm optimization (PSO) algorithm flowchart.

5. Conclusion:

In conclusion, leveraging Particle Swarm Optimization (PSO) to fine-tune the hyperparameters of Support Vector Regression (SVR) models emerges as a promising and effective strategy. By automating the parameter tuning process, PSO enhances SVR's predictive performance, particularly in complex and nonlinear regression contexts.

Looking ahead, hybrid optimization strategies—such as integrating PSO with other algorithms like genetic algorithms or grid search—could further improve the robustness and accuracy of SVR models. Moreover, applying PSO-optimized SVR to diverse domains—including genomics, finance, and smart grid systems—holds considerable potential to expand its practical utility and foster advancements in these fields.

Chapter 3
Results and Discussion

1. Introduction:

This chapter presents the experimental results derived from the application of the Support Vector Regression (SVR) model to enhance solar energy prediction, following the adjustment of its parameters using the Particle Swarm Optimization (PSO) algorithm. The primary objective of this chapter is to analyze the model's experimental performance and interpret the obtained results in the context of the adopted methodology.

Initially, the research methodology is reviewed, encompassing the steps of data collection, preprocessing, and partitioning into training, testing, and validation datasets. The evaluation criteria employed to assess the model's accuracy, including Root Mean Square Error (RMSE), Mean Absolute Error (MAE), Coefficient of Determination (R^2), and Mean Absolute Percentage Error (MAPE), are also detailed.

Subsequently, the optimization results obtained through the application of the PSO algorithm are presented and analyzed, with a comparison between the performance of the SVR model in its default state and its performance following optimization.

2. Definition of a Time Series:

Time series consist of collections of data organized in a specific temporal sequence. Generally, these values or events are measured, observed, or recorded at successive time intervals, which may or may not be evenly spaced. The data in a time series can be numerical, such as stock prices, daily temperatures, or monthly sales figures, or textual, such as diaries or interview transcripts, each tied to distinct points in time.

The temporal nature of time series is crucial, as it allows the data to be indexed according to time, providing a dynamic context that evolves over time.

$$Y_t = f(x_t, x_{t-1}, x_{t-2}, \dots \dots, x_{t-n}) \tag{3.1}$$

This equation illustrates this relationship, where the value at time t depends on past values and an error term. Time series analysis is widely employed across various disciplines, including economics, environmental science, meteorology, epidemiology, and more, to examine trends, model phenomena, and make predictions.

3. Data Sources:

The data for this study was gathered from the Adrar region, situated in southern Algeria. Adrar is distinguished by its hot desert climate and is renowned for its consistently high levels of solar irradiance throughout the year, making it an optimal location for solar energy research.

The dataset comprises time series measurements of solar radiation, potentially alongside other meteorological variables such as ambient temperature, humidity, wind speed, and atmospheric pressure. These variables play a crucial role in enhancing the precision of solar energy predictions. The figure 3.1 shows the location of the Wilaya of Adrar in Algeria.

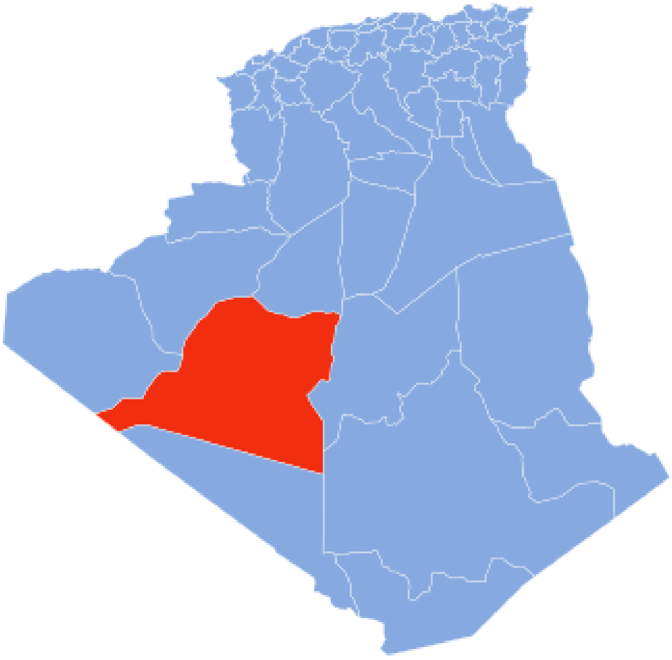

Figure 3.1: Location of the Wilaya of Adrar[42].

Table 3.1: The Statistical information of datasets.

Location	Horizon Time	Period	Statistical information			
			Max	**Min**	**STD**	**Mean**
Adrar	30 min	1/1/2016 to 31/12/2016	2.0533	-1.1686	1.0000	-3.1663e-16

The database for the Adrar site is presented in Figure 3.2.

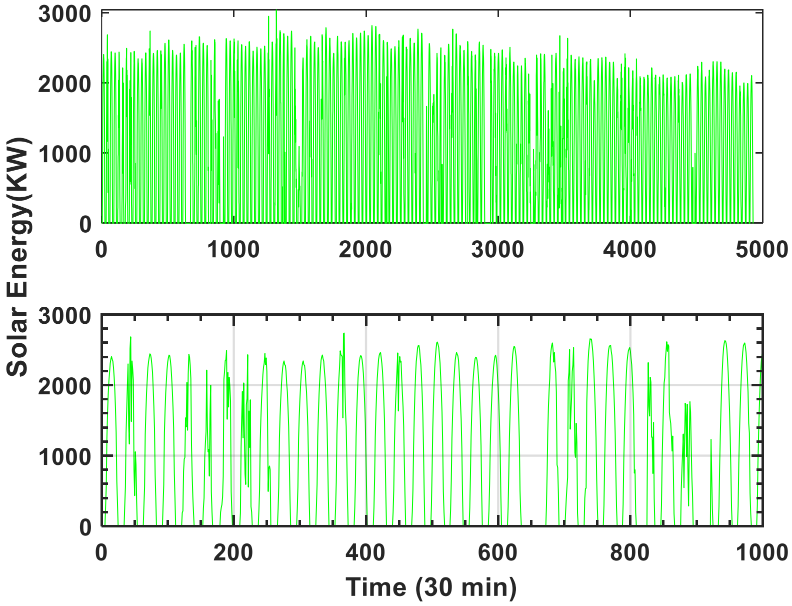

Figure 3.2: Adrar site database

4. Performance Evaluation Metrics:

4.1 Mean absolute error (MAE):

It is the mean of the total absolute difference between the values that were expected and those that were observed. It should be noted that MAE does not differentiate between the direction of the performance mistake; that is, it does not reveal whether the model is doing too well or too poorly. It may be computed as follows [24]:

$$\text{MAE} = \frac{1}{n}\sum_{i=1}^{n}\left|y_i - y_{pred}\right| \tag{3.2}$$

Where $y_i$is actual value and $y_{pred}$is the predicted value

4.2 Mean Squared Error (MSE):

Mean squared error (MSE) is quite comparable to mean absolute error (MSE), with the sole distinction being that MSE calculates the average of the sum of the squares of the variation between the initial and anticipated values. MSE has the benefit of making gradient computation simpler. Mean absolute error, on the other hand, computes the gradient using complex linear programming methods. The model may now concentrate more on the bigger mistakes as the influence of larger errors becomes more noticeable than that of smaller errors when we take the square of the error. It may be computed as follows: [24]

$$\text{MSE} = = \frac{1}{n}\sum_{i=1}^{n}(y_i - y_{pred})^2 \tag{3.3}$$

4.3 Root Mean Squared Error (RMSE):

The RMSE is the square root of the mean squared error (MSE), representing the standard error for normally distributed errors. The MSE and MAE are averaged forms of the L2 norm and L1 norm, respectively. Both are used in meteorology, air quality, and climate research studies, but there is no consensus on the most appropriate metric for model errors [43]

$$\text{RMSE} = \sqrt{\frac{1}{n}\sum_{i=1}^{n}(y_i - y_{pred})^2} \tag{3.4}$$

4.4 Coefficient of Determination (R^2):

The coefficient of determination, orR^2 metric, is typically used for explanatory purposes and indicates how well the predicted values fit the actual output values. It is commonly understood that R2 measures how well the model replicates the observed outcomes [24]

$$R^2 = 1 - \frac{SSres}{SStot} \tag{3.5}$$

Where:

. SS_{res} : is the residual sum of squares.

. SS_{tot} is the total sum of squares.

5. Particle Swarm Optimization (PSO)

Particle Swarm Optimization (PSO) is an evolutionary computation technique inspired by the collective behavior of birds and fish. It is commonly employed to address optimization problems, particularly in the context of parameter tuning in machine learning.

In this study, PSO is utilized to optimize the hyperparameters of the Support Vector Regression (SVR) model, specifically: C (the penalty parameter), ε (the epsilon-tube), and γ (the kernel coefficient for the Radial Basis Function (RBF) kernel).

6. Discussion of Results

6.1 Before PSO Optimization

Prior to applying the Particle Swarm Optimization (PSO) algorithm, the Support Vector Machine (SVM) models were configured with a set of initial parameters. These parameters were chosen based on standard values commonly used for each type of kernel. Table 3.2 outlines the parameter settings before the optimization process.

Table 3.2: Parameters used before PSO

	Gam	Sig	T	Degree
SVM_RBF	350	200		
SVM_Poly	350		2	
SVM_Lin	350		2	2

Before applying the Particle Swarm Optimization (PSO) algorithm, the performance of the different SVM models was evaluated using several evaluation metrics. The results obtained for each model are presented in Table 3.3, highlighting the RMSE, MAPE, R^2, and MABE values for the initial parameter settings.

Table 3.3: Results obtained before PSO

	RMSE	MAPE	R^2	MABE
SVM_RBF	0.1996	1.7819	0.9475	0.0151
SVM_Poly	0.2279	14.0399	0.9314	0.0137
SVM_Lin	0.2047	13.6899	0.9445	0.0023

The results presented in Table 3.3 show the performance of the different Support Vector Machine (SVM) models before the application of Particle Swarm Optimization (PSO). The performance is evaluated using four key metrics: Root Mean Square Error (RMSE), Mean Absolute Percentage Error (MAPE), R-squared (R^2), and Mean Absolute Bias Error (MABE).

- **SVM_RBF** (Radial Basis Function Kernel) yielded the best performance in terms of RMSE (0.1996) and R^2 (0.9475), indicating a strong fit to the data with relatively low error.

Its MAPE value (1.7819) suggests that the model was able to predict the solar radiation values with high accuracy, particularly when compared to the other models.

- **SVM_Poly** (Polynomial Kernel) exhibited a higher RMSE (0.2279) and MAPE (14.0399), which points to a less effective model in terms of predictive accuracy. The R² value of 0.9314 indicates a reasonably good fit, but the high MAPE suggests that the model has greater variability in its predictions compared to the others.
- **SVM_Lin** (Linear Kernel) produced moderate results, with an RMSE of 0.2047 and an R² of 0.9445. Its MAPE value of 13.6899 indicates a relatively higher error compared to the SVM_RBF model, but the model still provides reasonable accuracy. The very low MABE value (0.0023) indicates minimal bias in its predictions.

Overall, the **SVM_RBF** model demonstrated superior performance before optimization, providing the most accurate predictions with the least error. However, the results for **SVM_Poly** and **SVM_Lin** highlight that there is room for improvement in their accuracy and prediction consistency. The next step is to optimize these models using PSO to further enhance their performance.

6.2 After PSO Optimization

After applying Particle Swarm Optimization (PSO) to adjust the parameters of the Support Vector Machine (SVM) models, the optimized values for the parameters Sigma and Epsilon are presented in Table 3.4. These optimized parameters were found to significantly enhance the performance of each model.

Table 3.4: Optimized parameters

	Sigma_PSO	Epsilon_PSO
SVM_RBF	138.8025	2.1288
SVM_Poly	176.6864	4.2676
SVM_Lin	75.5723	

The table 3.5 presents the results obtained after the application of Particle Swarm Optimization (PSO) to the Support Vector Machine (SVM) models. The evaluation metrics—RMSE, MAPE, R², and MABE—are provided for each model after optimization.

Table 3.5: Results obtained after PSO

	RMSE	MAPE	R^2	MABE
SVM_RBF	0.1879	12.9463	0.9534	0.1015
SVM_Poly	0.2254	13.9019	0.9329	0.1089
SVM_Lin	0.2046	13.6898	0.9446	0.0023

The results obtained after the application of Particle Swarm Optimization (PSO) show varying degrees of improvement in the performance of the different Support Vector Machine (SVM) models. The performance is evaluated based on the RMSE, MAPE, R^2, and MABE metrics, and the following analysis provides a detailed look at how each model performed after optimization.

- **SVM_RBF**:

After PSO optimization, the **SVM_RBF** model demonstrates a notable improvement in performance. The **RMSE** decreased from 0.1996 to 0.1879, indicating a reduction in prediction error. Additionally, the **R²** value increased from 0.9475 to 0.9534, suggesting that the optimized model explains a higher proportion of variance in the data, which reflects better fitting and accuracy. However, the **MAPE** increased to 12.9463, significantly higher than its pre-optimization value (1.7819), which indicates more variability in the predictions despite the overall improvement in model accuracy. The **MABE** value also increased to 0.1015, pointing to a higher level of bias in the optimized model.

- **SVM_Poly**:

For the **SVM_Poly** model, the improvements after PSO optimization are marginal. The **RMSE** slightly improved from 0.2279 to 0.2254, and the **R²** increased slightly from 0.9314 to 0.9329, indicating a slight enhancement in model fit. However, the **MAPE** value increased to 13.9019, which is even higher than the pre-optimization value (14.0399), suggesting that the model’s predictions are still not very stable, with substantial variability in the results. Additionally, the **MABE** value (0.1089) increased, indicating a slight rise in the bias of the model after optimization.

- **SVM_Lin**:

The **SVM_Lin** model showed little change in performance after PSO optimization. The **RMSE** remained almost the same, with a slight decrease from 0.2047 to 0.2046. The **R²** value was virtually unchanged, increasing only slightly from 0.9445 to 0.9446. The **MAPE** and **MABE** values remained almost identical to the pre-optimization results, indicating no significant improvement or deterioration in prediction accuracy or bias. This suggests that PSO optimization had minimal impact on the **SVM_Lin** model’s performance.

For an overall assessment, we can conclude that: **SVM_RBF** emerged as the most improved model after PSO optimization, showing a reduction in error and an increase in the model fit (R^2), although there was some increase in prediction variability (MAPE) and bias (MABE). **SVM_Poly** showed slight improvement but continued to have significant variability in its predictions (high MAPE), indicating that the model's optimization was not highly effective.

SVM_Lin demonstrated minimal changes after optimization, suggesting that the linear kernel did not benefit significantly from the PSO adjustments.

Figure 3.3 provides a visual comparison between the real observed values, the predictions made by the standard SVM-RBF model, and the predictions of the PSO-optimized SVM-RBF model. Before PSO optimization, the curve representing the standard SVM-RBF model shows a good overall fit with the real values, but with noticeable deviations, especially during peaks or sharp drops in the data. This aligns with the pre-optimization results shown in **Table 3.3**, where the RMSE was 0.1996 and MAPE was 1.7819%, indicating that while the model provided reasonably accurate predictions, there was room for improvement, particularly in handling extreme values.

After PSO optimization, the curve for the PSO-optimized SVM-RBF model exhibits closer alignment with the actual values, particularly in regions with previously large errors. This improvement corresponds to the reduced RMSE (0.1879) and increased R² (0.9534), as shown in **Table 3.5**, reflecting a better model fit. However, the higher MAPE (12.9463%) after optimization suggests that, although the model's overall accuracy improved, certain points still exhibit increased relative errors, likely due to PSO-induced adjustments that improved general prediction accuracy at the cost of some variability in specific regions of the time series.

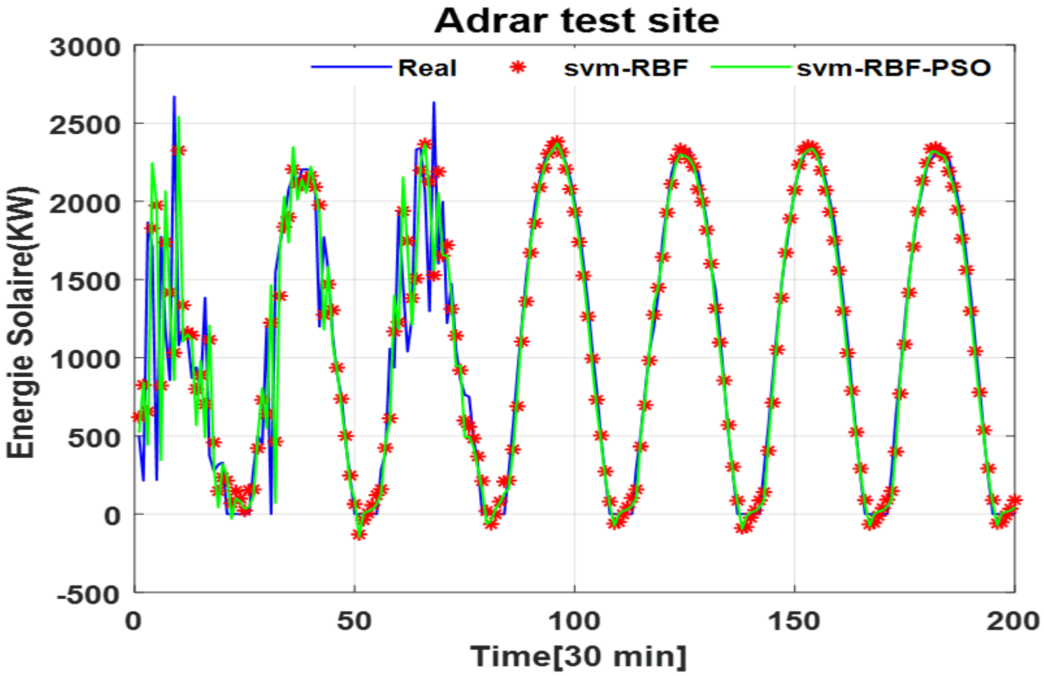

Figure 3.3: Comparison of Real Values, SVM-RBF, and PSO-Optimized SVM-RBF Predictions.

Figure 3.4 provides a visual comparison between the real observed values, the predictions made by the standard SVM-Poly model, and the predictions of the PSO-optimized SVM-Poly model. Before PSO optimization, the curve for the standard SVM-Poly model likely shows noticeable deviations from the actual values, particularly in areas with sharp changes or fluctuations in the data. This corresponds to the results presented in **Table 3.3**, where the RMSE was 0.2279 and MAPE was 14.0399%, indicating a higher level of prediction error and variability.

After PSO optimization, the curve for the PSO-optimized SVM-Poly model is expected to show closer alignment with the actual values, especially in regions where the pre-optimization model exhibited significant deviations. This improvement aligns with the results in **Table 3.5**, where the RMSE decreased to 0.2254 and the R^2 improved slightly to 0.9329. However, the higher MAPE (13.9019%) after optimization indicates that the model still exhibits considerable relative error, particularly in certain areas of the time series, reflecting that the optimization did not fully address prediction instability in those regions.

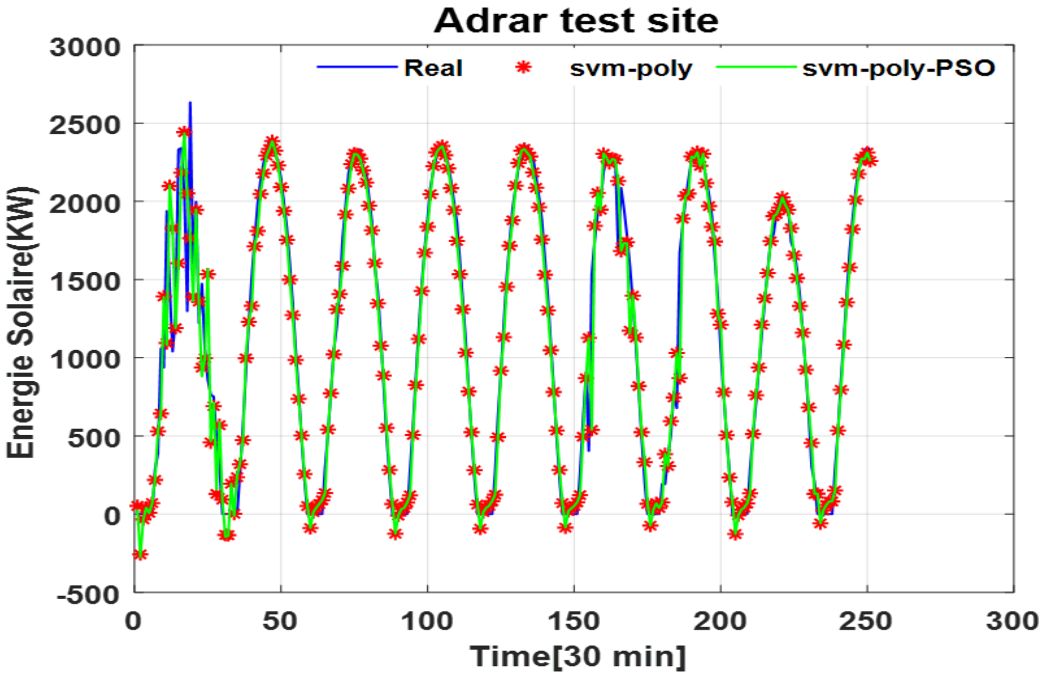

Figure 3.4: Comparison of Real Values, SVM-Poly, and PSO-Optimized SVM- Poly Predictions

Figure 3.5 provides a visual comparison between the real observed values, the predictions made by the standard SVM-Lin model, and the predictions of the PSO-optimized SVM-Lin model. Before PSO optimization, the curve for the standard SVM-Lin model likely shows a reasonable fit with the real values, but with some noticeable deviations, especially in regions with sharp changes in the data. This corresponds to the results in **Table 3.3**, where the RMSE was 0.2047 and MAPE was 13.6899%, indicating that the model had a moderate level of error, especially in capturing fluctuations.

After PSO optimization, the curve for the PSO-optimized SVM-Lin model is expected to show a similar alignment with the real values, with minimal changes in prediction accuracy, as the optimization did not significantly alter the performance of the model. This is in line with the results in **Table 3.5**, where the RMSE (0.2046) and MAPE (13.6898%) remained almost unchanged, and the R² (0.9446) showed no major improvement. The consistency in the performance suggests that the PSO optimization did not lead to significant improvements for the SVM-Lin model, reflecting its limited capacity for enhancement through the applied optimization process.

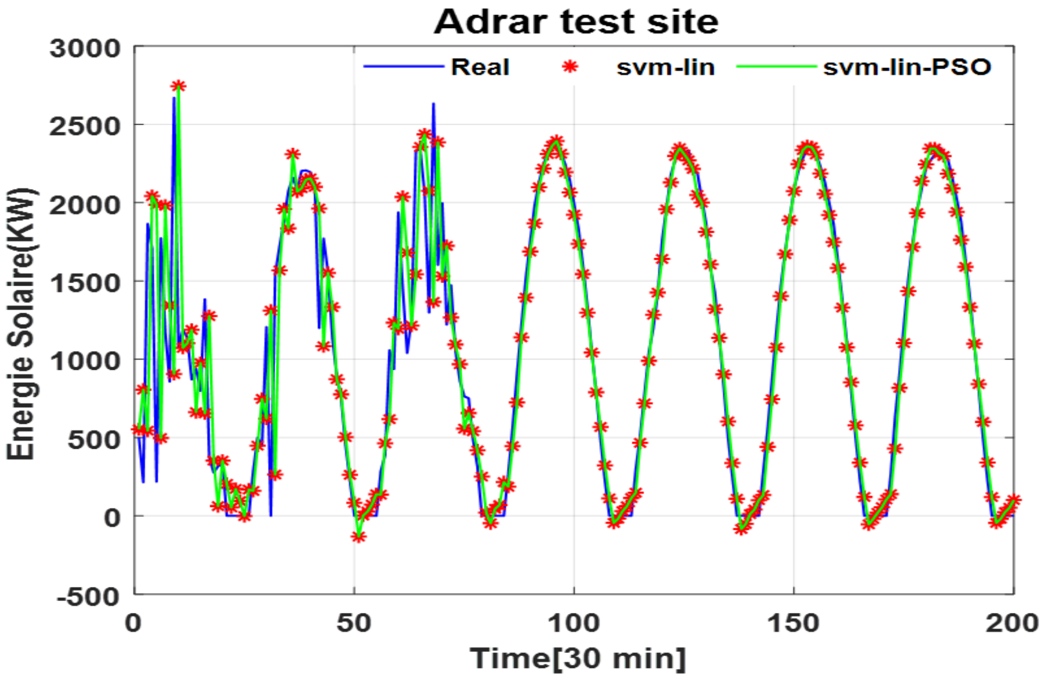

Figure 3.5: Comparison of Real Values, SVM-Lin, and PSO-Optimized SVM- Lin Predictions.

In conclusion, the analysis of the results before and after PSO optimization highlights the varying effectiveness of the optimization process across different SVM models. The **SVM-RBF** model demonstrated significant improvements, with reduced prediction errors (RMSE) and a better fit to the data (R²) after optimization, though the increased MAPE suggests that certain regions still exhibit higher relative errors. On the other hand, the **SVM-Poly** model showed slight improvements in terms of RMSE and R² but continued to struggle with high variability, as indicated by the high MAPE. Lastly, the **SVM-Lin** model experienced minimal changes after PSO optimization, showing that the linear kernel might not benefit as much from this optimization approach as the non-linear ones.

Overall, while PSO optimization improved the performance of the **SVM-RBF** model, the results suggest that the effectiveness of optimization varies depending on the kernel type, with non-linear models benefiting more than linear ones. These findings underscore the potential of using metaheuristic optimization techniques to enhance machine learning models for time series forecasting, but also highlight the need for further refinement when applied to certain models.

7.Conclusion:

In this study, we developed a hybrid forecasting model that combines Support Vector Regression (SVR) with Particle Swarm Optimization (PSO) to predict solar energy in the Adrar region. By optimizing the key hyperparameters of the SVR model, which is known for its strength in nonlinear regression tasks, the PSO algorithm enhanced its performance.

The PSO-optimized SVR model outperforms the standard SVR model, as evidenced by the improvements in the R^2, RMSE, and MAE metrics. This demonstrates the effectiveness of using metaheuristic optimization methods to enhance machine learning models for time series forecasting.

The proposed method offers a promising foundation for developing more advanced prediction models and could be applied to other regions and renewable energy types, providing valuable insights for future research and applications.

General conclusion

General conclusion

This dissertation presented the use of support vector regression (SVR) optimized by the particle swarm optimization (PSO) algorithm for solar energy forecasting at different forecast horizons. By applying this methodology to a case study at the Adrar site in Algeria, the results obtained show a significant improvement in forecast accuracy over traditional approaches. Integrating the optimization of SVR model hyper-parameters with PSO reduced prediction errors, confirming the effectiveness of this combination for the field of solar energy forecasting.

The work carried out in this dissertation has demonstrated that the use of advanced machine learning tools, such as SVR and PSO, represents a promising approach to solar energy management challenges. The results obtained are not only relevant to the Adrar region, but also applicable to other regions with similar climatic characteristics. This model could therefore be used to improve power grid management, optimize resources and facilitate the integration of solar energy into national energy systems.

However, there are some limitations to this study that open up interesting prospects for future research. Firstly, the modeling could be enriched by adding other climatic parameters, such as humidity or wind speed, which could have an impact on solar energy production. In addition, extending the study to other geographical sites and using real-time data would further refine the model's accuracy.

In addition, PSO optimization could be compared with other optimization methods, such as genetic algorithms or bee swarm optimization, to determine which technique offers the best performance for longer-term forecasts. Another avenue of research would be to integrate this approach into real-time energy management systems, thereby optimizing the use of solar energy in smart grids.

In conclusion, this work paves the way for better management of renewable energy resources in Algeria and elsewhere. The optimization of solar energy forecasts, using machine learning and optimization methods, is part of an approach aimed at fostering energy transition and promoting more sustainable solutions for a more resilient energy future.

BIBLIOGRAPHY

BIBLIOGRAPHY

[1] Y. . Z. Q. . & L. J. Liu, “Support vector machine-based prediction of solar power generation,” *Renew. Energy*, vol. 130, pp. 1022–1030, 2019.

[2] Z. . W. H. . & L. X. Zhang, “Hyper-parameter optimization of support vector regression using particle swarm optimization for solar power forecasting,” *Energy*, vol. 192, 2020.

[3] A. Harjanne and J. M. Korhonen, “Abandoning the concept of renewable energy,” *Energy Policy*, vol. 127, pp. 330–340, Apr. 2019, doi: 10.1016/j.enpol.2018.12.029.

[4] A. M. Klepacka, “SIGNIFICANCE OF RENEWABLE ENERGY SOURCES IN SUSTAINABLE DEVELOPMENT,” *Ann. Polish Assoc. Agric. Agribus. Econ.*, vol. XXI, no. 1, pp. 55–64, Mar. 2019, doi: 10.5604/01.3001.0013.0852.

[5] “Overview and key findings – World Energy Investment 2024 – Analysis - IEA.” Accessed: May 18, 2025. [Online]. Available: https://www.iea.org/reports/world-energy-investment-2024/overview-and-key-findings

[6] M. M. Rahman, K. Alam, and E. Velayutham, “Reduction of CO2 emissions: The role of renewable energy, technological innovation and export quality,” *Energy Reports*, vol. 8, pp. 2793–2805, Nov. 2022, doi: 10.1016/j.egyr.2022.01.200.

[7] “Renewable Energy: Global Challenges.” Accessed: May 18, 2025. [Online]. Available: https://www.e-ir.info/2016/05/27/renewable-energy-global-challenges/

[8] “Photovoltaic Effect - an overview | ScienceDirect Topics.” Accessed: May 18, 2025. [Online]. Available: https://www.sciencedirect.com/topics/engineering/photovoltaic-effect

[9] F. Kreith and R. T. Meyer, “Solar Thermal Conversion,” 1976.

[10] K. Alam Khan, S. Paul, M. Kamrul Alam Khan, A. Zobayer, and S. Sifat Hossain, “A Study on Solar Thermal Conversion,” *Artic. Int. J. Sci. Eng. Res.*, vol. 4, 2013, [Online]. Available: http://www.ijser.org

[11] M. Zeman, “PHOTOVOLTAIC SYSTEMS 9.1 Components of a PV system”.

[12] H. L. Zhang, J. Baeyens, J. Degrève, and G. Cacères, “Concentrated solar power plants: Review and design methodology,” 2013, *Elsevier Ltd*. doi: 10.1016/j.rser.2013.01.032.

[13] D. Gayen, R. Chatterjee, and S. Roy, “A review on environmental impacts of renewable energy for sustainable development,” Mar. 01, 2024, *Institute for Ionics*. doi: 10.1007/s13762-023-05380-z.

[14] Z. Bouzid, “Overview of solar potential, state of the art and future of photovoltaic installations in Algeria,” 2015. [Online]. Available: https://www.researchgate.net/publication/282981731

[15] C. Parekh, “Algeria Renewable Energy National Plan,” 2023, doi:

10.13140/RG.2.2.12417.84324.

[16] "Solar and Wind Energy Development in Algeria: Challenges and Future Prospects (2000-2030)." [Online]. Available: https://www.researchgate.net/publication/389853181

[17] M. D. Oisamoje and E. E. Oisamoje, "Exploring the Economic and Environmental Benefits of Solar Energy Generation in Developing Countries: The Nigerian Perspective", Accessed: May 19, 2025. [Online]. Available: www.iiste.org

[18] F. Yulianto, W. Firdaus Mahmudy, and A. A. Soebroto, "Comparison of Regression, Support Vector Regression (SVR), and SVR-Particle Swarm Optimization (PSO) for Rainfall Forecasting," 2020. [Online]. Available: www.jitecs.ub.ac.id

[19] M. A. Poole and P. N. O'farrell, "The assumptions of the linear regression model."

[20] F. Sohil, M. U. Sohali, and J. Shabbir, "An introduction to statistical learning with applications in R," *Stat. Theory Relat. Fields*, vol. 6, no. 1, pp. 87–87, 2022, doi: 10.1080/24754269.2021.1980261.

[21] M. Tranmer, J. Murphy, M. Elliot, and M. Pampaka, "Multiple Linear Regression (2 nd Edition)," 2020. [Online]. Available: https://hummedia.manchester.ac.uk/institutes/cmist/a

[22] G. K. Smyth, A. H. El-Shaarawi, and W. W. Piegorsch, "Nonlinear regression".

[23] "Efficient Learning Machines".

[24] "Machine Learning Algorithms", doi: 10.1007/978-3-030-71270-9_2.

[25] S. Gunn, "Support Vector Machines for Classification and Regression," 1997.

[26] H. Yu and S. Kim, "SVM tutorial-classification, regression and ranking," in *Handbook of Natural Computing*, vol. 1–4, Springer Berlin Heidelberg, 2012, pp. 479–506. doi: 10.1007/978-3-540-92910-9_15.

[27] T. O. Owolabi, K. O. Akande, S. O. Olatunji, N. Aldhafferi, and A. Alqahtani, "Modeling energy band gap of doped TiO2 semiconductor using homogeneously hybridized support vector regression with gravitational search algorithm hyper-parameter optimization," *AIP Adv.*, vol. 7, no. 11, Nov. 2017, doi: 10.1063/1.5009693.

[28] J. Kivinen, A. J. Smola, and R. C. Williamson, "Online Learning with Kernels," *IEEE Trans. SIGNAL Process.*, vol. 100, no. 10, 2010.

[29] M. V. Suganyadevi and C. K. Babulal, "Support Vector Regression Model for the prediction of Loadability Margin of a Power System," *Appl. Soft Comput. J.*, vol. 24, pp. 304–315, 2014, doi: 10.1016/j.asoc.2014.07.015.

[30] D. Basak, S. Pal, and D. C. Patranabis, "Support Vector Regression," 2007.

[31] E. Naranjo Bejarano Tutor and E. J. Carrizosa Priego, "Kernels Methods in Machine Learning".

[32] A. Dhankhar, S. Juneja, A. Juneja, and V. Bali, “Kernel Parameter Tuning to Tweak the Performance of Classifiers for Identification of Heart Diseases,” *https://services.igi-global.com/resolvedoi/resolve.aspx?doi=10.4018/IJEHMC.20210701.oa1*, vol. 12, no. 4, pp. 1–16, Jan. 1AD, doi: 10.4018/IJEHMC.20210701.OA1.

[33] “SVR — scikit-learn 1.6.1 documentation.” Accessed: May 16, 2025. [Online]. Available: https://scikit-learn.org/stable/modules/generated/sklearn.svm.SVR.html

[34] D. Wang, D. Tan, · Lei Liu, and L. Liu, “Particle swarm optimization algorithm: an overview”, doi: 10.1007/s00500-016-2474-6.

[35] N. K. Jain, U. Nangia, and J. Jain, “A Review of Particle Swarm Optimization”, doi: 10.1007/s40031-018-0323-y.

[36] G. Calas, “Optimisation par essaim particulaire”.

[37] S. Sengupta, S. Basak, and R. A. Peters, “Particle Swarm Optimization: A Survey of Historical and Recent Developments with Hybridization Perspectives,” Dec. 01, 2019, *MDPI*. doi: 10.3390/make1010010.

[38] “Mémoire OPTION Contrôle industriel Par BELLOUMI Rabie Optimisation par Essaim de Particules Application à un système complexe.”

[39] Y. del Valle, G. K. Venayagamoorthy, S. Mohagheghi, J. C. Hernandez, and R. G. Harley, “Particle swarm optimization: Basic concepts, variants and applications in power systems,” Apr. 2008. doi: 10.1109/TEVC.2007.896686.

[40] H. S. Salem, M. A. Mead, and G. S. El-Taweel, “Particle Swarm Optimization-Based Hyperparameters Tuning of Machine Learning Models for Big COVID-19 Data Analysis,” *J. Comput. Commun.*, vol. 12, no. 03, pp. 160–183, 2024, doi: 10.4236/jcc.2024.123010.

[41] G. F. Fan, L. L. Peng, X. Zhao, and W. C. Hong, “Applications of Hybrid EMD with PSO and GA for an SVR-Based Load Forecasting Model,” *Energies 2017, Vol. 10, Page 1713*, vol. 10, no. 11, p. 1713, Oct. 2017, doi: 10.3390/EN10111713.

[42] “Wilaya d’Adrar — Wikipédia.” Accessed: May 30, 2025. [Online]. Available: https://fr.wikipedia.org/wiki/Wilaya_d%27Adrar

[43] T. O. Hodson, “Root-mean-square error (RMSE) or mean absolute error (MAE): when to use them or not,” *Geosci. Model Dev*, vol. 15, pp. 5481–5487, 2022, doi: 10.5194/gmd-15-5481-2022.